

University of Alberta

Structure and Function Studies of ABCG1

by

Ge Li

A thesis submitted to the Faculty of Graduate Studies and Research
in partial fulfillment of the requirements for the degree of

Master of Science

in

Medical Sciences-Pediatrics

©Ge Li

Fall 2013

Edmonton, Alberta

Permission is hereby granted to the University of Alberta Libraries to reproduce single copies of this thesis and to lend or sell such copies for private, scholarly or scientific research purposes only. Where the thesis is converted to, or otherwise made available in digital form, the University of Alberta will advise potential users of the thesis of these terms.

The author reserves all other publication and other rights in association with the copyright in the thesis and, except as herein before provided, neither the thesis nor any substantial portion thereof may be printed or otherwise reproduced in any material form whatsoever without the author's prior written permission.

Abstract

ATP-binding cassette transporter G1 (ABCG1) mediates sterol efflux onto lipidated lipoproteins and plays an important role in macrophage cholesterol homeostasis. In this project, we investigated how ABCG1 works as a functional transporter to mediate sterol translocation. First, we found a conserved sequence present in the five ABCG transporter subfamily members. The conserved sequence locates between the nucleotide binding domain and the transmembrane domain and contains five amino acid residues from Asn at position 316 to Phe at position 320 in ABCG1 (NPADF). Detailed mutagenesis study revealed that Asn316 and Phe320 in the conserved sequence played an important role in the regulation of ABCG1 function. We further demonstrated that mutations N316D, N316Q and F320I led to retention of the protein in the endoplasmic reticulum (ER). Thus, the two highly conserved amino acid residues, Asn and Phe, may regulate ABCG1 trafficking, thereby affecting ABCG1-mediated cholesterol efflux. Second, we found a Stat3 binding site (YXXQ) located in the N-terminal cytoplasmic region of ABCG1. Replacement of Tyr at position 157 with Ala essentially eliminated ABCG1-mediated efflux of cholesterol and 7-ketocholesterol. On the other hand, substitution of Gln at position 160 with Ala affected the substrate specificity of ABCG1, reducing 7-ketocholesterol efflux with no significant effect on cholesterol efflux. In summary, we identified residues in the N-terminal cytoplasmic region of ABCG1 important for ABCG1 trafficking, function and substrate specificity.

Acknowledgments

The work within this dissertation was performed in the laboratory of Dr. Dawei Zhang in the Department of Pediatrics at the University of Alberta, Edmonton, Canada.

First and foremost, I owe the deepest gratitude to my mentor Dr. Dawei Zhang. His tremendous guidance, encouragement, passion and wisdom have always inspired, supported and motivated me throughout my graduate years. I am very grateful for the endless trust and all the opportunities he has given me to help me explore and challenge my potentials. Dr. Zhang guided me how to question thoughts and express ideas. His patience and support helped me overcome many crisis situations and helped me finish this dissertation. For everything you have done for me, Dawei, thank you.

I am also grateful to the former members of the Zhang laboratory that I have worked with – Xia Gao and Huashi Haziya. I am especially grateful to the current members, Hongmei Gu, Ayinuer Adijiang, and Faqi Wang, for their scientific discussions and their collaboration. Special thanks go out to all the members of molecular and cell biology of lipid group, for their helpful advice over the years.

I am very fortunate to have had great members on my committee – Dr. Richard Lehner and Dr. Elaine Leslie. I am deeply grateful for their input, valuable discussions and accessibility.

Finally, I would like to thank my husband An Zeng. His support, encouragement, patience and unwavering love have helped me stay strong and

optimistic throughout the graduate career. I would like to express my heart-felt gratitude to my parents, Shaomei Wang and Jinyi Li, for always encouraging me to pursue my dreams. They are the most wonderful parents anyone can wish for. They have been a constant source of love, support and strength all these years.

Table of Contents

CHAPTER 1 BACKGROUND AND INTRODUCTION	1
CHOLESTEROL TRANSLOCATION AND ABC TRANSPORTER	2
ABCG1 AND CHOLESTEROL HOMEOSTASIS.....	7
THE CURRENT STUDIES	13
CHAPTER 2 EXPERIMENTAL PROCEDURES	16
MATERIALS	16
CDNA CLONING OF ABCG1 AND SITE-DIRECTED MUTAGENESIS	17
CELL CULTURE AND GENERATION OF STABLE CELL LINES.....	19
CHOLESTEROL EFFLUX ASSAY	19
IMMUNOFLUORESCENCE OF ABCG1	20
BIOTINYLATION OF CELL SURFACE PROTEINS	21
PREPARATION OF MEMBRANE VESICLES FROM SF9 INSECT CELL.....	22
GEL FILTRATION OF ABCG1.....	23
SDS-PAGE AND IMMUNOBLOT ANALYSIS OF ABCG1	24
PULSE-CHASE ANALYSIS OF ABCG1 SYNTHESIS IN CULTURED CELLS	25
ATPASE ASSAY	26
STATISTICS.....	27
CHAPTER 3 IDENTIFICATION OF A CONSERVED SEQUENCE IN ATP BINDING CASSETTE TRANSPORTER G1 REGULATING PROTEIN TRAFFICKING AND FUNCTION	28
BACKGROUND.....	28
RESULTS.....	30
Effect of the conservative sequence on ABCG1 function.....	30
Roles of individually amino acid residues in the conserved sequence.....	35

Effect of mutations of Asn316 and Phe320 on the dimerization of ABCG1	41
Effects of mutations on ABCG1 trafficking.....	46
Effect of mutations on the ATPase activity of ABCG1	51
Effect of mutation on the stability of ABCG1.....	53
DISCUSSION.....	56
 CHAPTER 4 IDENTIFICATION THE FUNCTIONAL ROLES OF A STAT3	
BINDING SEQUENCE IN ATP BINDING CASSETTE TRANSPORTER G1	
BACKGROUND.....	61
RESULTS.....	67
The association between STAT3 and ABCG1	67
Effect of the STAT3 binding sequence on ABCG1 function.....	69
Effect of Y157A and Q160A on the dimerization of ABCG1	71
Effects of Y157A and Q160A on ABCG1 trafficking	73
Effect of Y157A and Q160A on the stability of ABCG1	77
Effect of Y157A and Q160A on ATPase activity of ABCG1.....	77
DISCUSSION.....	82
 CHAPTER 5 GENERAL CONCLUSION AND DISCUSSION	
REFERENCE	
APPENDICES	

List of Tables

Table 1 Primers for site mutagenesis	113
Table 2 QuikChange amplification reaction conditions	115

List of Figures

Figure 1. The major pathway of reverse cholesterol transport.	4
Figure 2. Schematic of ABC proteins.	6
Figure 3. Effect of the conservative sequence on ABCG1 function.	32
Figure 4. Role of individual residues within the conserved sequence in ABCG1-mediated cholesterol efflux.	37
Figure 5. Effect of wild type and mutant ABCG1 on ABCG1-mediated 7-ketocholesterol efflux.	39
Figure 6. Effects of mutations of N316D and F320I on ABCG1 dimerization.	43
Figure 7. Gel filtration chromatography of wild type and mutant ABCG1.	44
Figure 8. Trafficking of wild type and mutant ABCG1 in HEK293 cells.	47
Figure 9. Immunofluorescence localization of ABCG1 in stably transfected HEK 293 cells.	50
Figure 10. ATPase activity of ABCG1 in sf9 cell membrane vesicle.	52
Figure 11. Metabolic labeling of cells with ³⁵ S Cys/Met.	54
Figure 12. The predicted STAT3 binding site of ABCG1.	66
Figure 13. Immunoprecipitation of ABCG1.	68
Figure 14. Effect of mutations on ABCG1-mediated sterol efflux.	70
Figure 15. Effects of mutations of Y157A and Q160A on ABCG1 dimerization.	72
Figure 16. Biotinylation of Y157A and Q160A in HEK293 cells.	74
Figure 17. Immunofluorescence localization of wild type and mutant ABCG1 in stably transfected HEK 293 cells.	75
Figure 18. Metabolic labeling of cells with ³⁵ S Cys/Met.	79

Figure 19. ATPase activity of ABCG1 in sf9 cell membrane vesicle. 81

List of Abbreviations

7-KC	7-ketocholesterol
ABC	ATP-binding cassette transporter
ABCA1	ATP binding cassette transporter A1
ABCB11	ATP binding cassette transporter B11
ABCG1	ATP binding cassette transporter G1
ABCG4	ATP binding cassette transporter G4
ABCG5	ATP binding cassette transporter G5
ABCG8	ATP binding cassette transporter G8
Ala	Alanine
Asn	Asparagine
Asp	Aspartic acid
ATP	Adenosine-5'-triphosphate
apoA-I	Apolipoprotein A-I
apoA-II	Apolipoprotein A-II
apoB-100	Apolipoprotein B-100
apoE	Apolipoprotein E
BeFx	Beryllium fluoride
BSA	Bovine serum albumin
CE	Cholesteryl ester
CETP	Cholesteryl ester transfer protein
CVD	Cardiovascular disease
Cys	Cysteine

DAPI	4' 6-diamidino-2-phenylindole
DMEM	Dulbecco's modified Eagle's medium
DTBP	Dimethyl 3, 3'-dithiobispropionimidate
DTT	Dithiothreitol
ECs	Endothelial cells
ECL	Chemiluminescence
eNOS	Endothelial nitricoxide synthase
ER	Endoplasmic reticulum
FBS	Fetal bovine serum
FCS	Fetal calf serum
FC	Free cholesterol
Gln	Glutamine
GM-CSF	Granulocyte-macrophage colony-stimulating factor
HDL	High density lipoprotein
HEK	Human embryonic kidney
HEPES	4-(2-hydroxyethyl)-1-piperazineethanesulfonic acid
HMG-CoAR	Hydroxymethylglutaryl CoA reductase
HRP	Horseradish peroxidase
IL	Interleukin
Ile	Isoleucine
INSIG1	Insulin induced gene 1
JAK2	Janus kinase 2
LCAT	Lecithin: cholesterol acyltransferase

LCFA	Long chain fatty acids
LDL	Low density lipoprotein
LDLR	Low density lipoprotein receptor
LPL	Lipoprotein lipase
LPS	Lipopolysaccharide
LXR	Liver X receptor
LXRE	LXR response elements
MSDs	Membrane-spanning domains
Met	Methionine
NBDs	Nucleotide- binding domains
NO	Nitric oxide
PBS	Phosphate buffered saline
PBS-CM	PBS with 0.1 mM CaCl ₂ and 1mM MgCl ₂
pHDL	HDL purified from human plasma
Phe	Phenylalanine
PM	Plasma membrane
RCT	Reverse cholesterol transport
SCAP	Sterol regulatory element-binding protein cleavage-activating protein
SDS-PAGE	Sodium dodecyl sulfate polyacrylamide gel electrophoresis
Ser	Serine
SR-BI	Scavenger receptor B I

SREBP	Sterol regulatory element binding protein
STAT3	Signal transducer and activator of transcription 3
TCA	Trichloroacetic acid
Tfr	Transferrin receptor
TM	Transmembrane
VLDL	Very low density lipoprotein
TMD	Transmembrane domain
Tyr	Tyrosine
WHO	World health organization
WT	Wild type

Chapter 1 Background and introduction

Atherosclerotic cardiovascular disease is defined as diseases and injury of the cardiovascular system and characterized by the accumulation of cholesterol and triglyceride in the arterial wall (Oram and Vaughan, 2006).

Although the cardiovascular disease death rate in Canada has declined by more than 75 percent since 1952 and nearly 40 percent in the last decade, every 7 minutes in Canada, someone dies from heart disease or stroke (Statistics Canada, 2011). Heart disease and stroke are two of the three leading causes of death in Canada and cost the Canadian economy more than \$20.9 billion every year in physician services, hospital costs, lost wages and decreased productivity (Conference Board of Canada, 2010). Atherosclerosis is caused by a variety of factors including genetics and lifestyle. Poor diet, deficiency in physical activity, and tobacco consumption are the major environmental influences that contribute to heart disease. High blood pressure, high blood cholesterol, obesity, and the chronic disease of type 2 diabetes are among the major biological risk factors (WHO). Nine in 10 Canadians (90%) have at least one risk factor for heart disease or stroke (smoking, alcohol, physical inactivity, obesity, high blood pressure, high blood cholesterol, diabetes) (Public Health Agency of Canada, 2009).

Coronary heart disease, stroke, hypertension, heart failure, and rheumatic heart disease are major types of cardiovascular diseases. Currently, several drugs are used to lower the high risk of heart attack and stroke recurrence and death. Statins are used for lowering blood cholesterol, and aspirin may help patients with

an elevated risk of heart attack and stroke by daily taken. However, heart disease is still a major public health concern. Atherosclerosis is one major cause of heart disease. Two major hallmarks of atherosclerosis are inflammation and the deposition of excess cholesterol in arterial macrophages. In this thesis, the latter is the major focus.

Cholesterol translocation and ABC transporter

Cholesterol is an essential structural component of mammalian cell membranes, establishing both proper membrane permeability and fluidity. In addition, cholesterol is also involved in cell signaling processes and is an important component for the synthesis of bile acids, steroid hormones and some vitamins. However, accumulation of excess cholesterol is toxic to cells. The dysregulation of cholesterol metabolism is a critical factor in the development of coronary atherosclerosis, which is one of the leading causes of death in Canada as discussed above. In addition, aberrant cholesterol trafficking and accumulation is the molecular basis for other disorders such as Tangier's disease, and Alzheimer's disease (Berge et al., 2000; Brooks-Wilson et al., 1999; Hollingworth et al., 2011; Orso et al., 2000).

Cholesterol homeostasis in humans is regulated by well-balanced mechanisms of intestinal uptake, endogenous synthesis and metabolism, transport in lipoprotein particles, and biliary excretion. In mammals, all nucleated cells can synthesize cholesterol, however, none of these cells have the capacity to degrade cholesterol. To maintain cholesterol homeostasis, any surplus of cholesterol must either be stored in the cytosol in the form of esters or released from the cell. The

liver plays a critical role in regulating cholesterol homeostasis since it is the only organ that can convert cholesterol to bile acids and excrete cholesterol directly into the bile. Typically, removal of excessive cholesterol from peripheral cells is accomplished through the so-called reverse cholesterol transport (RCT) pathway (Rosenson et al., 2012; Wang et al., 2007). The major steps in RCT (Figure 1) include: acquiring cholesterol from peripheral cells by acceptors such as apolipoprotein A-I (apoA-I) and high density lipoprotein (HDL), the esterification of free cholesterol in HDL by the plasma enzyme lecithin: cholesterol acyltransferase, and the transport of cholesteryl ester from HDL to apoB containing lipoproteins by the cholesteryl ester transfer protein for the eventual delivery to the liver where it can be excreted directly into the bile or converted to bile acids prior to excretion. Recently, a group of ATP-binding cassette (ABC) transporters has been shown to play critical roles in the RCT pathway by mediating the translocation of cholesterol across cellular bilayer membranes (Brooks-Wilson et al., 1999; Kobayashi et al., 2006; McNeish et al., 2000; Rosenson et al., 2012; Singaraja et al., 2002; Singaraja et al., 2006; Vaughan and Oram, 2005, 2006; Wang et al., 2004).

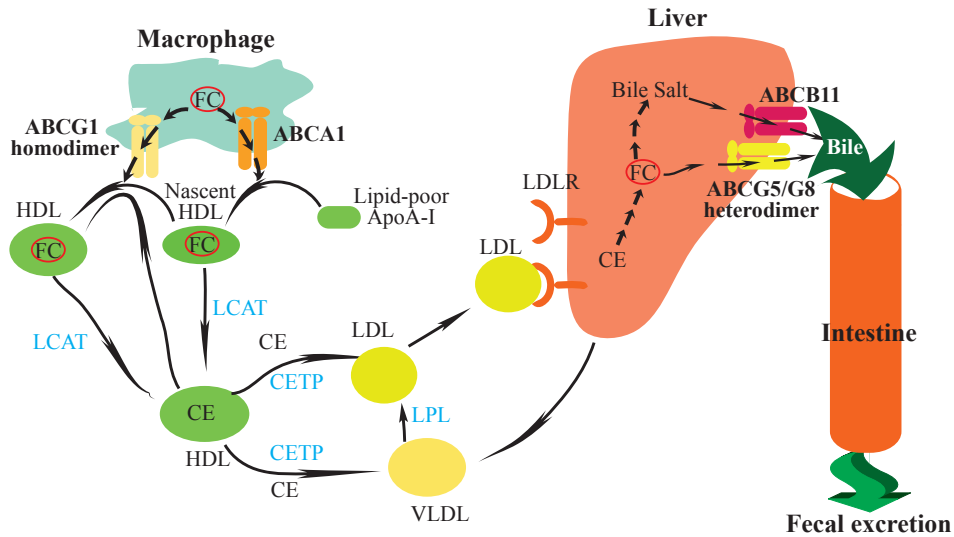


Figure 1. The major pathway of reverse cholesterol transport.

- 1) Acquiring free cholesterol (FC) from peripheral cells by acceptors such as apolipoprotein A-I (apoA-I) and HDL through ABCA1 and ABCG1, respectively;
 - 2) the esterification of free cholesterol in HDL by the plasma enzyme lecithin: cholesterol acyltransferase (LCAT) and the transport of cholesteryl ester (CE) from HDL to apo-B containing lipoproteins by the cholesteryl ester transfer protein (CETP);
 - 3) the uptake of CE by the liver;
 - 4) the conversion of CE to FC and bile salt in the liver;
 - 5) the excretion of FC and bile salt into bile via ABCG5/G8 and ABCB11, respectively for the final fecal excretion or recycling.
- LPL: lipoprotein lipase.

The ABC superfamily of transporters comprises a large family of functionally diverse polytopic transmembrane proteins. Most ABC transporters share a common molecular architecture that includes two nucleotide-binding domains (NBDs) arranged in series with two membrane-spanning domains (MSDs). So far, 48 ABC superfamily genes have been identified in the human genome that can be further divided into 7 subfamilies (ranging from ABCA to ABCG). The functional transporter can either be a single protein with two NBDs and two MSDs (a full transporter) or be a homo- or hetero-dimer consisting of two half transporters (Figure 2). The MSD of typical ABC transporters contains 6 transmembrane alpha-helices, which form the putative channel for substrates across the lipid bilayer and are believed to define the substrate specificity for each transporter. Thus, the MSDs vary considerably between different ABC proteins. In contrast, the NBDs of the ABC transporters are highly conserved. Each NBD contains three highly conserved sequence elements (the Walker A and B motifs and a signature motif, Figure 2) that play critical roles in nucleotide binding and hydrolysis and in the provision of energy for the transporter to translocate its substrates across the cell membranes.

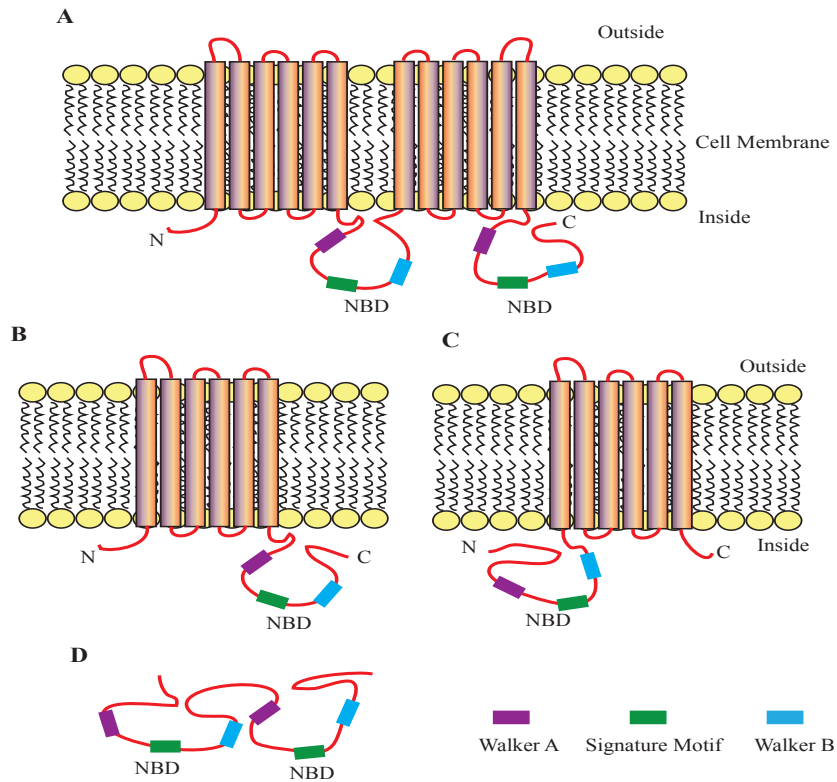


Figure 2. Schematic of ABC proteins.

Panel A: The schematic structure of a typical mammalian full ABC transporter consisting of two MSDs and two NBDs. Panels B and C: The schematic structure of a typical mammalian half ABC transporter containing one MSD and one NBD at the C-terminus (B) or N-terminus (C). Panel D: The schematic structure of mammalian ABC proteins in the 'F' subfamily containing two NBDs and no MSD.

ABC transporters utilize energy derived from ATP binding/hydrolysis at NBDs to translocate a wide variety of substrates including amino acids, lipids, inorganic ions, peptides, saccharides, metals, drugs, and proteins across extra- and intracellular biological membranes. Mutations in several human ABC transporter genes have been linked to 16 genetic diseases (Moitra and Dean, 2011). ABC transporters play critical roles in lipid transport and metabolism. For example, ABCA1 mediates the efflux of cholesterol and phospholipids from peripheral cells onto apoA-I in the initial stages of RCT (Brooks-Wilson et al., 1999; McNeish et al., 2000; Orso et al., 2000; Singaraja et al., 2002; Singaraja et al., 2006). ABCG5 and ABCG8 participate in the excretion of cholesterol and plant sterols into bile and into the gut lumen (Berge et al., 2000; Yu et al., 2002a; Yu et al., 2002b). ABCG1 mediates cellular cholesterol export to lipidated lipoprotein particles (Kobayashi et al., 2006; Vaughan and Oram, 2005; Wang et al., 2004; Wang et al., 2007).

ABCG1 and cholesterol homeostasis

ABCG1 belongs to the 'G' branch of the ABC transporter superfamily. The putative structure of the 'G' branch consists of six TM alpha helices and one NBD at the N-terminus (Figure 2C) (Dean, 2002; Higgins, 2007; Sharom, 2008). Some of the G family members, such as ABCG1 and ABCG2, function as homodimers (Engel et al., 2006; Leimanis and Georges, 2007), whereas other family members, such as ABCG5 and ABCG8, function as heterodimers (Graf et al., 2003). ABCG1 is ubiquitously expressed, with relatively high expression levels in the

spleen, lung, brain, and kidneys (Kennedy et al., 2005). ABCG1 is also highly expressed in human macrophages where it can be upregulated by liver X receptor (LXR) agonists and cholesterol loading (Beyea et al., 2007; Kennedy et al., 2001), but suppressed by lipid efflux (Abildayeva et al., 2006). Transfection of ABCG1 in cultured cells or up-regulation of the expression of endogenous ABCG1 in several cell types increases the efflux of cellular cholesterol to HDL or to lipidated apoA-I but not to lipid-free apoA-I (Sano et al., 2007; Vaughan and Oram, 2005; Wang et al., 2004). On the other hand, inhibition of *ABCG1* expression in several cell lines results in reduced HDL-dependent efflux of cholesterol and phospholipid from these cells (Klucken et al., 2000). Most recently, it has been reported that knockdown of the transcriptional co-regulator, GPS2, expression essentially abolishes LXR-induced *ABCG1* expression in human macrophage THP-1 cells and dramatically reduces HDL-mediated cholesterol efflux from the cells while having no effect on *ABCA1* expression (Jakobsson et al., 2009). However, Larrede *et al* (Larrede et al., 2009) reported that knockdown of *ABCG1* expression in THP-1 cells had no significant effect on LXR agonists-induced cholesterol efflux onto HDL. The reason for this difference is unclear.

Mice lacking ABCG1 accumulate lipids in macrophages and in hepatocytes (Kennedy et al., 2005), and show a significantly decreased level of plasma HDL after being fed a high cholesterol diet or treated with the LXR agonist T0901317 (Wiersma et al., 2009). Transgenic mice over-expressing the human *Abcg1* gene are protected against dietary fat-induced lipid accumulation in the liver and lungs

(Kennedy et al., 2005). Moreover, over-expression of *ABCG1* in macrophages significantly increases macrophage RCT *in vivo*, whereas knockdown or knockout of *ABCG1* expression markedly decreases macrophage RCT *in vivo* (Wang et al., 2007). Interestingly, several studies showed that ABCG1, but not ABCA1, is responsible for the reduction in macrophage cholesterol efflux in patients with type 2 diabetes mellitus, which contributes to the reduction in cholesterol efflux in macrophages (Mauldin et al., 2008; Mauldin et al., 2006). Similarly, ABCG1, but not ABCA1, is involved in the inhibition of foam cell formation induced by peroxisome proliferator-activated receptor-gamma agonists (Li et al., 2004). Rohrer *et al* (Rohrer et al., 2009) reported that ABCG1 and scavenger receptor BI (SR-BI), but not ABCA1, are responsible for the crossing of HDL through aortic endothelial cells. Moreover, the expression of *ABCG1* is upregulated in macrophages from patients with Tangier disease (Lorkowski et al., 2001), who have dysfunctional ABCA1 (Brooks-Wilson et al., 1999). These findings reveal the critical role of ABCG1 in cholesterol efflux onto HDL and indicate the linkage between the transporter and protection against atherosclerosis.

However, the precise role of macrophage ABCG1 in the protection against the development of atherosclerosis remains uncertain. Over-expression of *ABCG1* in *ApoE*^{-/-} mice fed a high-fat diet had no significant effect on atherosclerosis (Burgess et al., 2008), whereas transplantation of bone marrow lacking *Abcg1* into LDL receptor knockout (*Ldlr*^{-/-}) mice showed conflicting effects. Out *et al.* (Out et al., 2006) observed a moderate increase in atherosclerosis, consistent with the role of the transporter in promoting macrophage cholesterol efflux. However,

two other independent groups, Baldan *et al.* (Baldan et al., 2006) and Ranalletta *et al.* (Ranalletta et al., 2006) reported that macrophages lacking *ABCG1* leads to atherosclerosis in hyperlipidemic *Ldlr*^{-/-} mice. Ranalletta rationalized that the decrease in atherosclerosis results from the induction of *ABCA1* expression and increased apoE levels. Terasaka *et al* suggested that *ABCG1* deficiency in macrophages increase apoptosis, and this is supported by the finding that ABCG1 promotes the efflux of 7-ketocholesterol onto HDL, thereby protecting macrophages from oxysterol-induced apoptosis (Terasaka et al., 2007). However, Seres recently reported that overexpression of ABCG1 results in phosphatidyl serine (PS) translocation, caspase 3 activation, and subsequent cell death, suggesting that ABCG1 may be associated with apoptotic cell death in macrophages (Seres et al., 2008). To further determine the role of ABCG1 in atherosclerosis, Out *et al.* (Out et al., 2007) examined atherosclerotic lesion formation and development in *Abcg1*^{-/-} mice fed an atherogenic diet and found that ABCG1 indeed has a protective function in initial lesion formation. Westerterp *et al* reported that mice with vascular *ABCG1* deficiency show increased atherosclerotic lesion areas (Westerterp et al., 2010). More recently, it has been shown that lacking *ABCG1* in *Ldlr*^{-/-} mice increases early atherosclerotic lesions but delays the progression of advanced atherosclerotic lesions (Meurs et al., 2012). Thus, the precise role of ABCG1 in the development of atherosclerosis is complex.

ABCG1 is highly expressed in endothelial cells. The half transporter plays a critical role in the removal of cholesterol from endothelial cells and protects

against endothelial dysfunction. ABCG1 promotes cholesterol efflux from endothelial cells onto HDL, reduces cholesterol contents in caveolae and reverses the interaction between caveolin1 and endothelial NO synthase (eNOS), consequently leading to increased eNOS activity (Terasaka et al., 2010). Furthermore, ABCG1 localizes to the membranes of insulin granules in pancreatic β cells and is involved in insulin secretion. The expression of ABCG1 in islet is significantly reduced in diabetic mice. ABCG1 deficiency dramatically reduces pancreatic β cell insulin secretion in mice (Sturek et al., 2010). Therefore, ABCG1-mediated cholesterol translocation plays various important physiological roles. Recently, several lines of evidence show that ABCG1 and ABCA1 can promote cellular cholesterol efflux synergistically in vitro (Gelissen et al., 2006; Vaughan and Oram, 2006). The efflux of cholesterol and phospholipids onto apoA-I mediated by ABCA1 converts apoA-I into nascent HDL, which can then act as an acceptor for ABCG1-mediated cholesterol efflux (Figure 1). Knockout of both *ABCA1* and *ABCG1* in mice leads to dramatic foam cell formation and acceleration of atherosclerosis (Yvan-Charvet et al., 2007). These findings demonstrate the combined, protective effects of ABCA1 and ABCG1 in the pathogenesis of atherosclerosis. ABCG1 and ABCA1 are also highly expressed in hematopoietic stem and multipotential progenitor cells. Knockout of both *ABCA1* and *ABCG1* in mice leads to leukocytosis. Studies by Yvan-Charvet *et al* revealed that ABCG1 and ABCA1-mediated cholesterol efflux reduces cell plasma membrane cholesterol content, which reduces cell surface levels of the β subunits of the interleukin 3 (IL-3) /granulocyte-macrophage colony-stimulating

factor (GM-CSF) receptor and consequently results in decreased proliferative responses to IL-3 and GM-CSF (Yvan-Charvet et al., 2010a).

How ABCG1 facilitates the movement of cholesterol across the bilayer membrane is unclear. Unlike ABCA1, ABCG1 does not directly bind to its acceptors such as HDL (Wang et al., 2004). It has been reported that ABCG1 redistributes cholesterol to the outer leaflet of the plasma membrane, which can be removed by HDL (Vaughan and Oram, 2005). Most recently, Tarling *et al* (Tarling and Edwards, 2011) reported that ABCG1 is an intracellular cholesterol transporter. They propose that ABCG1 transfers sterols to the inner leaflet of the intracellular vesicles, and then these vesicles fuse with the plasma membrane and deliver cellular cholesterol to exogenous HDL. ABCG1 has been shown to localize to intracellular endosomes (Tarling and Edwards, 2011) and the membranes of insulin granules in pancreatic β cells (Sturek et al., 2010). When overexpressed, the half transporter is localized to the endoplasmic reticulum (ER), Golgi, and plasma membranes (Gao et al., 2012; Gu et al., 2013; Kobayashi et al., 2006; Tarling and Edwards, 2011; Vaughan and Oram, 2005). Most recently, we have demonstrated that ABCG1 is palmitoylated at five cysteine residues located in the N-terminal cytoplasmic region. Disruption of palmitoylation at position 311 through mutation of Cys311 to Ala or Ser affects ABCG1 trafficking from the ER. Therefore, our data suggest that palmitoylation plays a critical role in ABCG1-mediated cholesterol efflux through the regulation of protein trafficking (Gu et al., 2013). In addition, we recently reported that a highly conserved His residue located in the putative first transmembrane domain of

ABCG1 is required for ABCG1-mediated cholesterol efflux (Gao et al., 2012). When reconstituted in phosphatidylserine liposome, the ATPase activity of ABCG1 is stimulated by cholesterol (Hirayama et al., 2012), indicating that ABCG1 may be an active cholesterol transporter. However, if ABCG1 directly binds to cholesterol and functions as an active cholesterol transporter or, like ABCA1, acts as a cholesterol efflux regulator remains the subject of ongoing investigation.

The current studies

My thesis project focused on delineating the molecular mechanism of ABCG1-mediated sterol efflux. One project was to study the role of a conserved motif (NPADF) located between the NBD and membrane-spanning domain in ABCG1. We found that, in addition to the traditional conserved motifs (the Walker A motif, the Walker B motif, and a signature motif) that are important for ATP binding and hydrolysis, there is a highly conserved sequence present in the ‘G’ branch of the ABC transporter superfamily. The sequence is located between the NBD and membrane-spanning domain and contains five amino acid residues. Asn, Pro, Asp and Phe are completely conserved among all the five ‘G’ subfamily members. The second project focused on studying the potential role of a signal transducer and activator of transcription 3 (STAT3) binding motif in ABCG1. STATs are a highly conserved family of transcription factors that have dual roles, as cytoplasmic signaling proteins and as nuclear transcription factors. Seven members of this family have been identified, including STAT1, STAT2, STAT3, STAT4, STAT5a, STAT5b and STAT6. Different members are involved in cell

proliferation, survival, differentiation, apoptosis or angiogenesis (Buettner et al., 2002; Levy and Darnell, 2002; Yu and Jove, 2004). STATs are activated in response to the binding of a large number of cytokines (interleukin (IL) family: IL-6, IL-2, IL-10 or interferon family), hormones (growth hormone and leptin) and growth factors (epidermal growth factor, insulin growth factor or platelet-derived growth factor) to their receptors (Silva, 2004). Binding of a ligand to its receptor triggers dimerization of the cytoplasmic domain of the receptor and the juxtaposition and activation of associated Janus tyrosine kinases (JAKs 1, 2 and 3 or Tyk2), which subsequently phosphorylate STATs on their conserved tyrosine residue (Yu and Jove, 2004). Recent studies on ABCA1 revealed that ABCA1 interacts with STAT3 and functions as an anti-inflammatory receptor (Tang et al., 2009). The interaction of apoA-I with ABCA1 promotes cholesterol removal and activates a signaling molecule, STAT3, which is independent of the lipid transport function of ABCA1. ABCA1 contains two candidate STAT3 binding sites. The interaction of apoA-I with ABCA1-expressing macrophages suppresses the ability of lipopolysaccharide (LPS) to induce the production of several inflammatory cytokines including IL-1 β , IL-6, and tumor necrosis factor- α . Thus, the ABCA1 pathway functions as an anti-inflammatory in macrophages through the activation of STAT3 (Tang et al., 2009). These findings implicate that ABCA1 acts as a direct molecular link between the cardioprotective effects of cholesterol export from arterial macrophages and suppresses inflammation. We found that ABCG1 also contains a conserved STAT3 binding site (YXXQ) in its N-terminal cytoplasmic region. The STAT3 binding site contains four amino acid residues,

Tyr157, Ile158, Met159 and Gln160, in which Tyr 157 and Gln160 are required for the integrity of a STAT3 binding site.

My projects focused on investigating the potential roles of the highly conserved motif, NPADF and the STAT3 binding motif in ABCG1 function. To do so, we first replaced these highly conserved amino acid residues with Ala. Human embryonic kidney293 (HEK293) cells transiently or stably overexpressing wild type or mutant ABCG1 were labeled with ³H sterols. The efflux of sterol onto lipidated apoA-I was examined. We found that mutations of Asn316 and Phe320 within the conserved sequence significantly affected ABCG1 function. Mutation of Tyr157 to Ala in the STAT3 binding motif also significantly reduced the efflux of cholesterol and 7-ketocholesterol. On the other hand, replacement of Gln160 with Ala in the STAT3 binding motif affected substrate specificity of ABCG1, reducing 7-ketocholesterol efflux without detectable effect on cholesterol efflux.

Chapter 2 Experimental procedures

Materials

Lipofectamine 2000 and Directional pCDNA3.1 TOPO vectors were obtained from Invitrogen. Culture medium, antibiotic G-418 sulfate, EZ Link Sulfo-NHS-LC-Biotin and Streptavidin-agarose slurry were purchased from Thermo Scientific. Complete EDTA-free protease inhibitors were purchased from Roche. Poly-D-lysine and fetal bovine serum (FBS), bovine serum albumin (BSA), horseradish peroxidase (HRP)-conjugated secondary antibodies (HRP-goat anti-mouse or HRP-donkey anti-rabbit IgG) were purchased from Sigma. [³H]-cholesterol (54.2 Ci/mmol) and [³⁵S]- Met/Cys were purchased from PerkinElmer (Waltham, MA). Polyclonal anti-ABCG1 antibodies were purchased from Novus Biologicals and Santa Cruz Biotechnology, Inc. Polyclonal anti-Calnexin antibody (used at 1:10,000 dilution) was purchased from BD Biosciences, and monoclonal anti-Transferrin receptor (Tfr) antibody (used at 1:5,000 dilution) was purchased from Abcam. IRDye Secondary antibodies (IRDye 800CW Goat anti-Rabbit IgG and IRDye 680 Goat anti-Mouse IgG) were purchased from Licor Biosciences. Quick Change Lightning Site-Directed Mutagenesis Kit was purchased from Agilent Technologies. Nitrocellulose membranes were purchased from Thermo Scientific and GE Healthcare, respectively.

The lipidated apoA-I used in these experiments contains a Myc-DDK tag at the C-terminus and was purified from HEK 293S cells as described (Zhang et

al., 2008). Briefly, HEK 293S cells stably expressing tagged human apoA-I were cultured in suspension in IS GRO serum-free medium (Irvine Scientific) supplemented with 10% FBS. ApoA-I was purified by anti-FLAG M2 affinity gel chromatography (Sigma) following the manufacturer's instruction. The lipidated fraction of apoA-I was isolated via size-exclusion chromatography on a Tricorn Superdex 200 10/300 column (GE Healthcare). Protein purity was monitored by sodium dodecyl sulfate polyacrylamide gel electrophoresis (SDS-PAGE) and protein staining using EZ-Run protein gel staining solution.

A custom-made rabbit polyclonal anti-ABCG1 antibody, 4497, was produced by Genscript using a peptide (TKRLKGLRKDSSSM, amino acids from 374 to 387 of ABCG1) as the antigen. 4497-conjugated beads were produced as followed: 20 ml of 50% slurry of protein A beads were washed with 50 ml of PBS 3-time. Then 10 mg purified antibody 4497 were applied to the beads and rotated gently for 1 h at room temperature. The beads were washed with 50 ml of 0.2 M sodium borate (pH 9.2) twice and resuspended in 50 ml of 0.2 M sodium borate. Solid dimethyl pimelimidate (final concentration: 20 mM, Sigma) were added to the beads and rotated at room temperature for 30 min. The reaction was stopped by washing beads once with 50 ml of 0.2 M ethanolamine (pH 8.0). Beads were then resuspended and incubated with 0.2 M ethanolamine at room temperature for 2 h. After three wash with PBS, the beads were resuspended with PBS containing 0.02% NaN₃ for later use.

cDNA cloning of ABCG1 and site-directed mutagenesis

Human ABCG1 cDNA cloned in this study was the same as the reported

canonical sequence (Gene Bank accession number: NM_004915.3) except that the first four amino acid residues (MACL) were missing in the cDNA that we used. The ABCG1 cDNA was cloned into Directional pcDNA3.1 TOPO vector alone (pcDNA3.1-ABCG1) or together with C-Myc or HA tag at the C-terminus (C-Myc or tagged ABCG1). The mutations were generated using the Quick Change Lightning Site-Directed Mutagenesis Kit according to the manufacturer's instructions. The template used was pcDNA3.1-ABCG1 or C-Myc/HA tagged ABCG1. Oligonucleotides bearing mismatched bases at the residue to be mutated were synthesized by IDT, Inc. (Coralville, IA) (see Appendix table 1). The sample reactions were set up at 25 μ l volume containing 2.5 μ l of 10 X reaction buffer, 50 ng of dsDNA template, 125 ng of forward oligonucleotide primer, 125 ng of reverse oligonucleotide primer, 0.5 μ l of dNTP mix, 0.75 μ l of Quick Solution reagent and 0.5 μ l of Quick Change Lightning Enzyme. The reaction conditions are listed in the Appendix Table 2.

The amplification reaction samples were then incubated with 1 μ l of *DpnI* restriction enzyme at 37°C for 2 h. *DpnI* treated DNA from each reaction sample was transformed into 50 μ l of DH5 α competent cells. DNA and competent cells were gently mixed and incubated on ice for 30min, and then the cells were heat shocked at 42°C for 45 sec, followed by incubation on ice for 2 min. With the addition of 1 ml of pre-warmed LB broth, the transformants were incubated at 37°C for 1 h with shaking at 250 rcf, and then selected on the agar plates containing antibiotic ampicillin (at 100 μ g/ml). The presence of the desired mutation and the integrity of each construct were verified by DNA sequencing

(TAGC, Edmonton, Canada).

Cell culture and generation of stable cell lines

HEK 293 cells were maintained in Dulbecco's modified Eagle's medium (DMEM) (Glucose, 4.5 g/liter) containing 10% (v/v) FBS, 100 units/ml penicillin, and 100 µg/ml streptomycin. Cells were cultured at a 37 °C with 5% CO₂ and 95% humidity. To generate the stable cell lines, HEK 293 cells were transfected with pcDNA3.1 or plasmids containing wild type or mutant ABCG1, and then selected by antibiotic G418. Specifically, HEK 293 cells were seeded at 5X10⁵ cells/well in a 6-well plate. After 24 h, the cells were transfected with empty vector, or cDNA construct containing wild type or mutant ABCG1 (3.2 µg/well), using Lipofectamine 2000 (8 µl/well). 4 h later, the medium were replaced with fresh DMEM containing 10% FBS. After reaching to 95% confluence, the cells were split and selected with 1 mg/mL antibiotic G-418 for over two weeks until there was no living cell observed in the control group (HEK 293 cells without transfection). The living cells were then cloned by limiting dilution in 96-well plates with DMEM medium containing 10% FBS and 1 mg/mL antibiotic G-418. Several subclones were isolated, and the expression of ABCG1 was confirmed by western blot analysis with a rabbit polyclonal anti-ABCG1 antibody (Novus). Those subclones stably overexpressing wild type or mutant ABCG1 were maintained in DMEM containing 10% FBS and 0.2 mg/mL G-418.

Cholesterol efflux assay

Cholesterol efflux assay was performed as described previously

(Kobayashi et al., 2006; Wang et al., 2004). For transient transfection, HEK 293 cells were seeded at 2.5×10^5 cells/well in a 12-well plate. After 24 h, the cells were transfected with plasmids expressing wild type or mutant ABCG1 (1.6 $\mu\text{g}/\text{well}$) using Lipofectamine 2000 (4 $\mu\text{l}/\text{well}$). For the cells stably overexpressing wild type or mutant ABCG1, the cells were seeded at 2.5×10^5 cells/well in a 12-well plate. 48 h later, the cells were directly labeled with [^3H]-cholesterol (2 $\mu\text{Ci}/\text{ml}$) for 16 h. Cells were then washed with 1 ml of DMEM containing 0.02% BSA and incubated at room temperature for 5 min, followed by a second wash, and incubated at 37°C for 30 min. After the third wash with 1 ml of DMEM containing 0.02% BSA, the cells were incubated with 5 $\mu\text{g}/\text{ml}$ lipidated apoA-I in DMEM containing 0.02% BSA for 5 h. The media were then collected and the cells were lysed in 0.5 ml of lysis buffer A (0.1 N NaOH, 0.01% SDS). The radioactive content of the media and cells was measured separately by scintillation counting (LS 6500 Multi-Purpose Scintillation Counter, Beckman Coulter). Sterol transfer was expressed as the percentage of the radioactivity released from the cells into the media relative to the total radioactivity in cells plus media. Data were analyzed with GraphPad Prism software and significance was defined as $p < 0.05$.

Immunofluorescence of ABCG1

Confocal microscopy was carried out as described previously (Zhang et al., 2001a, b; Zhang et al., 2007). Approximately 5×10^5 cells were seeded in each well of a 6-well tissue culture dish on coverslips. After 24 h, the cells were transfected with plasmids expressing wild type or mutant ABCG1 as described

previously. 48 h later, the cells were washed and fixed with 3% paraformaldehyde in phosphate buffered saline (PBS). The cells were permeabilized using methanol for 20 min, and washed with a blocking solution of 1% BSA in PBS. Then the cells were incubated overnight in a blocking solution containing an anti-ABCG1 polyclonal antibody, H-65 (used at 1:100 dilution). After washing with the blocking solution for 10 min, the cells were incubated with Alexa Fluor 488 goat anti-rabbit IgG for 1 h, followed by washing 3-times 10 min with blocking solution. Coverslips were mounted on slide with one drop of Anti-fade reagent containing 4', 6'-diamidino-2-phenylindole (DAPI) (Vector Laboratories, Burlingame, CA). Localization of ABCG1 in the transfected cells was determined using a Leica SP5 laser scanning confocal microscope (filters: 461 nm for DAPI, 488 nm for Fluor 488).

Biotinylation of cell surface proteins

Biotin labeling of cell surface proteins was carried out exactly as previously described (Zhang et al., 2008; Zhang et al., 2007). For transient transfection, HEK 293 cells were set up in a 6-well plate and transfected with plasmids expressing WT or mutant ABCG1 as described previously. For the cells stably overexpressing WT or mutant ABCG1, the cells were seeded at 5×10^5 cells/well in a 6-well plate. After 48h, HEK 293 cells overexpressing WT or mutant ABCG1 were washed twice with ice-cold PBS buffer, and then biotinylated using EZ-Link Sulfo-NHS-LC-Biotin, following the manufacturer's protocol (Thermo Scientific). Specifically, the cells were incubated with 0.5 mg/ml EZ-Link Sulfo-NHS-LC-Biotin in amine free PBS buffer with gently

rocking at 4°C for 30 min. The cells were then washed with cold PBS buffer twice, and the reaction was terminated by blocking with cold PBS containing 100 mM glycine for 20 min at room temperature. After 3 washes with PBS, the cells were lysed in 200 µl of lysis buffer B (1% triton, 150 mM NaCl, 50 mM Tris-HCl, pH 7.4). A total of 45 µl of the cell lysate was saved and 150 µl of the lysate was added to 60 µl of 50% slurry of NeutrAvidin-agarose (Thermo Scientific) and another 200 µl of lysis buffer B. The mixture was rotated overnight at 4°C. After centrifugation at 5204 rcf for 5 min, the pellets were washed three times with lysis buffer B by centrifugation at 5204 rcf for 5 min and the cell surface proteins were eluted from the beads by adding 60 µl of 2X SDS loading buffer (62 mM Tris-HCl, pH 6.8, 2% SDS, 50% glycerol, 0.005% bromphenol). A 15 µl of 4X SDS loading buffer was added to the saved 45 µl cell lysate, and both the cell lysates and cell surface proteins were incubated for 5 min at 85°C. Proteins were then subjected to SDS-PAGE (8% acrylamide) and analyzed by immunoblotting with a rabbit anti-ABCG1 polyclonal antibody (H-65, SantaCruz) and a mouse anti-calnexin polyclonal antibody (BD Biosciences).

Preparation of membrane vesicles from sf9 insect cell

Membrane vesicles were generated through nitrogen cavitation as described previously with minor modifications (Gao et al., 1996). Sf9 cells expressing WT or mutant ABCG1 were harvested in membrane buffer (250 mM sucrose, 50 mM Tris-HCl, pH 7.4). The cell pellets were stored at -80°C in membrane buffer containing 1X protease inhibitors. The cell pellets were thawed under hot water, EDTA was added to a final concentration of 0.5 mM. The cells

were then disrupted by nitrogen cavitation (equilibration at 250 p.s.i. for 10 min) on ice. After centrifugation at 1800 rpm for 10 min, the supernatants were laid over 35% (w/v) sucrose in 20 mM Tris-HCl, 0.5 mM EDTA and then centrifuged at 25000 rpm for 2 h (Beckman, Sw32 Ti). The white interface (~7 ml) was collected and washed once with the diluted membrane buffer (4 ml membrane buffer and 16ml double-distilled H₂O) through another centrifugation at 25000 rpm for 1 h. The membrane pellets were suspended in the membrane buffer and the samples were further passed through a 27-gauge needle for 10 strokes to generate membrane-enriched vesicles. The protein concentration of these membrane vesicles were determined using the BCA assay (Pierce). The membrane enriched vesicles were aliquoted and temporarily stored at - 80 °C for future studies.

Gel filtration of ABCG1

Gel filtration chromatography was performed on an AKTA explorer system (GE Healthcare) with a Superose-12 10/300 column. The cells stably expressing the wild type or mutant ABCG1 generated as previously described were solubilized in 500 µl of lysis buffer B containing 1X proteinase inhibitors and 10 mM dithiothreitol (DTT). The lysates were centrifuged for 15 min at 14,000 rpm to clear insoluble materials. The supernatant was injected into the column pre-equilibrated with 2 column volumes of the same lysis buffer. The elution was collected at 0.5 ml per fraction and fractions were precipitated with trichloroacetic acid solution (TCA, 6.1 N) overnight at 4°C. The samples were centrifuged for 10 min at 15,000 rpm. The pellets were then washed twice with

cold acetone and dried at 85°C for 30 min. The dried pellets were dissolved in 60 µl of 9 M urea. With the addition of 20 µl of 4X SDS loading buffer, the samples were subjected to SDS-PAGE and immunoblotting. The retention time of ABCG1 was determined by SDS-PAGE and immunoblotting of the collected fractions. Gel filtration protein standard including ferritin (670 kDa), aldolase (158 kDa), ovalbumin (44 kDa), myoglobin (17 kDa), and vitamin B12 (1.35 kDa) (GE Healthcare) were separated under the same condition and observed using a UV detector.

SDS-PAGE and immunoblot analysis of ABCG1

In cholesterol efflux experiments, the cells overexpressing WT or mutant ABCG1 were collected and lysed in the 1% Triton X-100 lysis buffer containing 1X complete EDTA-free protease inhibitors for 30 min. The samples were centrifuged for 10 min at 15,000 rpm. The supernatant was collected and subjected to 8% SDS-PAGE and transferred to nitrocellulose membranes (GE Healthcare). Immunoblotting was performed using an anti-ABCG1 polyclonal antibody (H-65, Santa Cruz). In sucrose gradient and gel filtration experiments, the fractions were precipitated with TCA and dissolved in 9 M of urea and separated by SDS-PAGE (8%, or 8% to 12%). After electrophoresis and electrotransferring, the membranes were analyzed by immunoblotting with a rabbit anti-ABCG1 polyclonal antibody (H-65), a rabbit anti-caveolin1 monoclonal antibody, and a mouse anti-transferrin (Tfr) monoclonal antibody. In biotinylation experiments, both the whole cell lysates and the pellets were subjected to 8% SDS-PAGE and transferred to nitrocellulose membranes

(GE Healthcare). Membranes were probed with both a rabbit anti-ABCG1 polyclonal antibody (H-65, Santa Cruz) and a mouse anti-calnexin polyclonal antibody,

To assess the above first antibody binding, membranes were either blotted with horseradish peroxidase (HRP)-conjugated goat anti-mouse or donkey anti-rabbit IgG (Sigma), followed by enhanced chemiluminescence (ECL) and then exposed to Kodak BioMax MR films; or probed with IRDye Secondary Antibodies (IRDye 800 CW Goat anti-Rabbit IgG and IRDye 680 Goat anti-Mouse IgG), followed by near-infrared fluorescence detection in an Odyssey infrared imaging system. For quantification studies of the gel filtration experiments, the detection was applied and the densitometry was analyzed with the Odyssey infrared imaging software.

Pulse-chase analysis of ABCG1 synthesis in cultured cells

Stable cell lines overexpressing WT or mutant ABCG1 were set up at the density of 1.2×10^6 cells / 5 ml in 60 mm petri dish. For each cell type, total 6 dishes were set up for 6 time points (0, 0.25, 0.5, 1, 2, and 4 h). After 48 h, the cells were washed twice with 10 ml of PBS-CM (PBS with 0.1mM CaCl₂ and 1mM MgCl₂) (37°C) and incubated in 4 ml of glutamine-, methionine-, and cysteine- free DMEM with 5% dialyzed fetal calf serum (FCS) and 2 mM glutamine for 30 min at 37°C. Newly translated proteins were metabolically labeled for 15 min at 37°C with 3.5 ml of glutamine-, methionine- and cysteine-free DMEM containing 5% dialyzed FCS and 2 mM glutamine containing 100 μ Ci/ml [³⁵S]- Met/Cys. The cells were then washed twice with PBS-CM (37°C)

and incubated with DMEM containing 10% FBS to all plates except the zero point samples for up to 4 h. Cells were collected at indicated time points, washed twice in 10 ml of ice-cold PBS-CM, and collected in 1 ml of ice-cold PBS. The cells were spun at 425 rcf for 5 min at 4 °C. The supernatant was removed. The cell pellets were lysed in 300 µl of 1% triton X-100 lysis buffer containing 1X complete EDTA-free protease inhibitors on ice for 30 min and spun for 10 min at 14,000 rpm at 4°C. The supernatant was collected for the whole cell lysates. Same amount of total proteins was applied to 60 µl of 4497-conjugated beads overnight at 4°C to immunoprecipitate ABCG1. The samples were centrifuged at 5204 rcf for 3 min. The supernatant was collected as immunoprecipitated supernatant. The beads were washed 3 times in 1 ml of lysis buffer B. The immunoprecipitated proteins were eluted from the beads by adding 60 µl of 2 X SDS loading buffer, followed by an incubation at 37 °C for 10 min. 25 µl of eluted samples was subjected to 8% SDS-PAGE in duplicate. One gel was used for Western Blot to detect ABCG1 protein levels. Another one was fixed in isopropanol / water / acetic acid (25: 65: 10) for 30 min, and then soaked in Amplify solution to enhance the ³⁵S-signal. The gel was then dried under vacuum, and exposed to Kodak BioMax MS film (Kodak, Rochester NY) for up to 24 h at - 80 °C.

ATPase assay

Membrane enriched vesicles made from sf9 cells were diluted to 0.5 µg/µl in the membrane buffer. Each sample was performed in triplicate in the presence and absence of BeFx. 2 X reaction buffer containing 50 mM HEPES (pH 7.0), 0.5 mM MgCl₂, 10 mM NaN₃, and 1mM EGTA was made freshly before each

experiment. 40 μ l of membrane and 10 μ l of diluted protein vesicles buffer were added into each well of a 96-well plate. 100 μ l of 2X reaction buffer were then added into each well. 1.5 μ l of 20 mM BeCl₂ and 1.5 μ l of 500 mM NaF were then added into BeFx plus group to form BeFx that inhibits ABCG1 ATPase activity. Samples were mixed by pipetting up and down four times and incubated at 37 °C for 10 min. Then, 10 μ l of 100 mM ATP was added into each well and samples were mixed by pipetting up and down four times before incubating at 37 °C for 1 h. Stop buffer was made fresh when 15 min of 1 h incubation were left. The ratio of buffer B (18% ascorbic acid in H₂O): buffer C (3 M HCl): buffer D (1.5% ammonium molybdate in H₂O): buffer A (18% SDS in H₂O) was 1:1:2:2. To make the stop buffer, buffer B and C were mixed first, and then buffer D was added. After briefly vortex, buffer A was added and mixed by pipetting up and down. The reactions were terminated with 100 μ l of stop buffer. 100 μ l of citrate: arsenite: HAc mixture (2% sodium citrate, 2% sodium arsenite and 2% acetic acid in H₂O) was then added into each well to stabilize the phosphomolybdate complex. After standing for 10 min, the absorbance was measured at 630 nm.

Statistics

Results were presented as the mean \pm S.D. Differences between groups were analyzed using unpaired Students *t*-test to evaluate levels of significance. Significance is defined as $p < 0.05$ (GraphPad Prism 5.0).

Chapter 3 Identification of a conserved sequence in ATP binding cassette transporter G1 regulating protein trafficking and function

Background

ABCG1 belongs to the 'G' branch of the ABC transporter superfamily that includes five half transporters, ABCG1, ABCG2, ABCG4, ABCG5 and ABCG8. The putative structure of the 'G' branch consists of one NH₂-terminal nucleotide binding domain (NBD) and one COOH-terminal membrane-spanning domain that contains 6 putative transmembrane α -helices (Figure 3A) (Dean, 2002; Higgins, 2007; Sharom, 2008). Some of the G family members, such as ABCG1 and ABCG2, function as homodimers (Engel et al., 2006; Leimanis and Georges, 2007), whereas other family members, such as ABCG5 and ABCG8, function as heterodimers (Graf et al., 2003). ABCG1 is localized to the endoplasmic reticulum (ER), Golgi and plasma membranes in macrophages and other cell types (Engel et al., 2006; Kobayashi et al., 2006; Vaughan and Oram, 2005; Xie et al., 2006). The half transporter mediates cholesterol efflux onto lipidated lipoproteins like HDL but not onto lipid poor apoA-I (Engel et al., 2006; Kobayashi et al., 2006; Vaughan and Oram, 2005; Wang et al., 2004; Wang et al., 2007). Mice lacking *Abcg1* accumulate lipids in macrophages and in hepatocytes (Kennedy et al., 2005), and show a significantly decreased level of plasma HDL after being fed a high cholesterol diet or treated with the LXR agonist T0901317 (Wiersma et al., 2009).

ABCG1 is highly expressed in macrophages and plays an important role in macrophage reverse cholesterol efflux *in vivo*. Overexpression of ABCG1 in macrophages significantly increases macrophage reverse cholesterol transport (RCT) *in vivo*, whereas knockdown or knockout of *Abcg1* expression in macrophages markedly decreases macrophage RCT *in vivo* (Wang et al., 2007). However, the precise role of macrophage ABCG1 in the protection against the development of atherosclerosis remains uncertain. Transplantation of bone marrow lacking *Abcg1* into LDL receptor knockout (*Ldlr*^{-/-}) mice showed conflicting effects. Out *et al.* (Out et al., 2006) observed a moderate increase in atherosclerosis, whereas two other independent groups reported that macrophages lack of ABCG1 decrease in atherosclerosis in hyperlipidemic *Ldlr*^{-/-} mice (Baldan et al., 2006; Ranalletta et al., 2006). What accounts for this difference is unclear.

ABCG1 and ABCA1 have been shown to promote cellular cholesterol efflux synergistically (Gelissen et al., 2006; Vaughan and Oram, 2006). The efflux of cholesterol and phospholipids onto apoA-I mediated by ABCA1 converts apoA-I into nascent HDL, which can then act as an efficient acceptor for G1-mediated cholesterol efflux. It has been demonstrated that ABCA1 and ABCG1, but not scavenger receptor BI (SR-BI), are responsible for macrophage RCT *in vivo* and that the effects of ABCA1 and ABCG1 on promoting cholesterol efflux are synergistically (Wang et al., 2007). Knockout of both *ABCA1* and *ABCG1* in mice leads to dramatic foam cell formation and acceleration of atherosclerosis (Out et al., 2008a; Out et al., 2008b; Yvan-Charvet et al., 2007). Most recently, it has been showed that ABCG1-mediated cholesterol translocation

plays an important role in pancreatic β -cell insulin secretion (Fryirs et al., 2010; Kruit et al., 2012; Sturek et al., 2010). ABCG1 is required for reconstituted HDL-promoted insulin secretion. The Lack of ABCG1 expression both *in vivo* and *in vitro* dramatically reduced insulin secretion. However, how ABCG1 mediates cholesterol efflux is unclear.

We have identified one highly conserved cysteine residues located at position 514 (Cys514) in the first putative transmembrane α -helix that plays an important role in ABCG1-mediated cholesterol efflux. Replacement of Cys514 with Ala or Ser essentially eliminated ABCG1-mediated cholesterol efflux (Gao et al., 2012). The transmembrane domains of the ABC transporters vary considerably between different ABC proteins. In contrast, the NBDs of the ABC transporters are relatively hydrophilic and highly conserved. Each NBD contains three highly conserved sequence elements (the Walker A motif, the Walker B motif, and a signature motif) that play critical roles in nucleotide binding and hydrolysis and in provision of energy for the transporter to translocate its substrates across the cell membranes.

Results

Effect of the conservative sequence on ABCG1 function

The 'G' subfamily members are different from other ABC transporters. The 'G' subfamily members contain an NH₂-terminal NBD. Sequence analysis showed that there is one highly conserved sequence, Asn (N), Pro (P), Ala (A),

Asp (D), and Phe (F), present in all ABCG family members except for ABCG5, in which it is NPFDF (Figure 3A). Here, we mutated these amino acid residues to investigate their potential roles in ABCG1-mediated sterol efflux. N316, P317, D319 and F320 in ABCG1 were replaced with Ala simultaneously (NPDF-A). Cholesterol efflux assay was performed on HEK 293 cells transiently expressing wild type or mutant ABCG1. As shown in Figure 3C, the expression level of NPDF-A was comparable to that of the wild type protein. However, mutation NPDF-A virtually eliminated ABCG1-mediated cholesterol efflux (Figure 3D). Thus, the conserved sequence plays an important role in ABCG1 function.

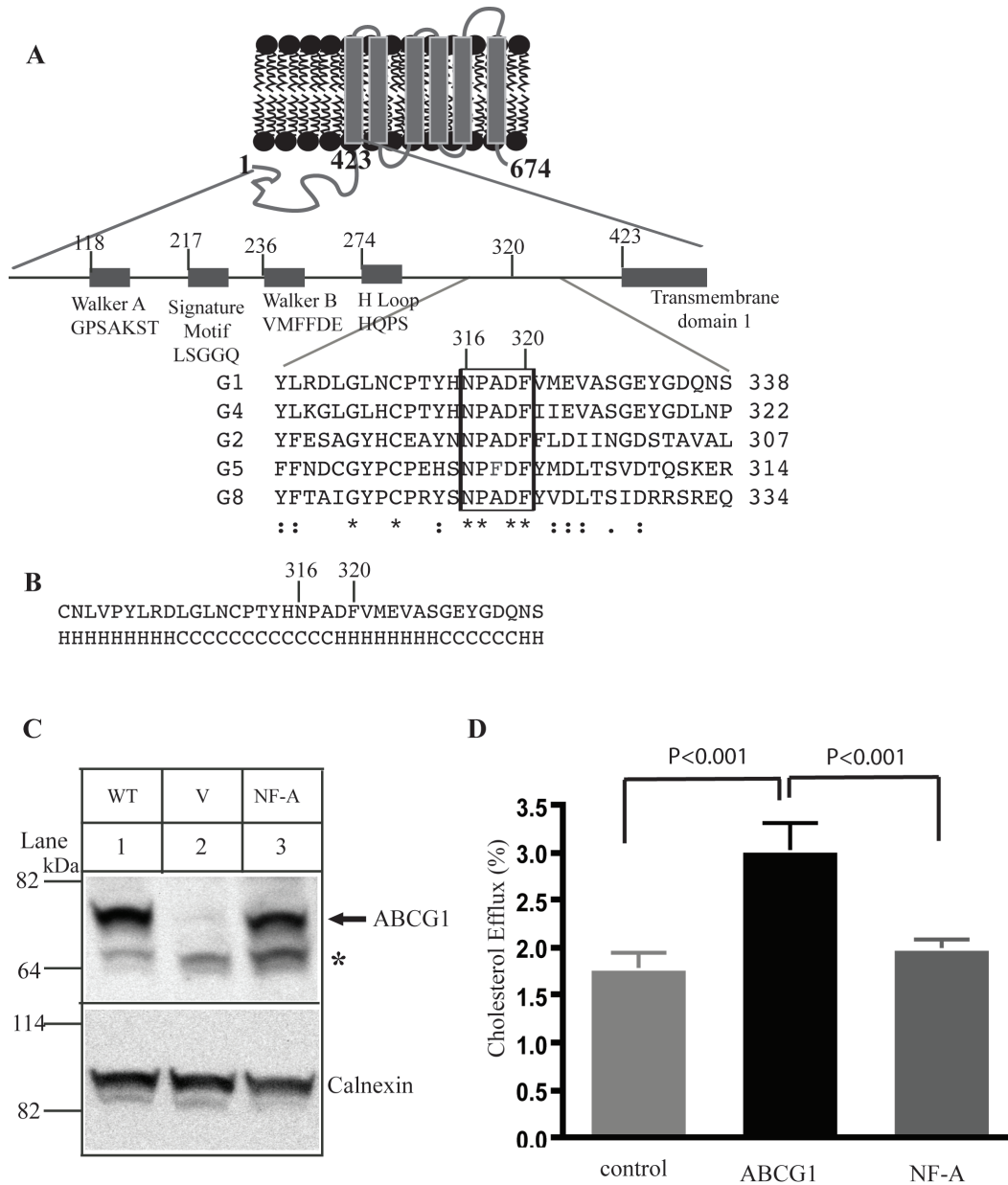


Figure 3. Effect of the conservative sequence on ABCG1 function.

Panel A: Predicted topology of ABCG1 and sequence alignment for ABCG family. Only part of sequence alignment that includes the conserved sequence (NPADF) was shown. The sequence alignment was performed using ClustalW2.

Panel B: The predicted secondary structure of the linker region between NBD and the transmembrane domain in ABCG1. Several secondary structure algorithms

provided from ExPASy (www.expasy.ch/tools) including GOR, Jpred3, SOPMA, and Psipred were used to predict the secondary structure. Only part of the predicted secondary structure that includes the conserved sequence (NPADF) was shown. H, alpha helix. C, random coil. Panel C: Expression of wild type and mutant ABCG1 in HEK 293 cells transiently overexpressing wild type and mutant ABCG1. Whole cell lysates were made from HEK293 cells transiently transfected with empty vector (V) or vectors containing wild type ABCG1 (WT) or mutant ABCG1 (NPADF-A) cDNA and subjected to SDS-PAGE and immunoblotting. The membrane was cut into halves along the 82 kDa based on the pre-stained protein standards (Life technology). Membrane containing proteins in the 64-82 kDa mass was probed with a polyclonal anti-ABCG1 antibody, H-65 (Santa Cruz) and membrane containing protein in the 82-114 kDa mass was detected with a polyclonal anti-calnexin antibody. Antibody binding was detected using HRP-conjugated goat anti-mouse or with donkey anti-rabbit IgG (Sigma), followed by enhanced ECL detection (Pierce). The membranes were then exposed to Kodak BioMax MR films (Kodak). Panel D. Cholesterol efflux. ABCG1-mediated cholesterol efflux onto lipidated apoA-I was carried out as described. HEK293 cells were transiently transfected with empty vector (control) or plasmid containing cDNA of wild type or mutant ABCG1, NF-A, in which N316, P317, D319 and F320 were replaced with Ala simultaneously. The cells were then labeled with ³H-cholesterol. After washing, the cells were incubated with 5 µg/ml lipidated apoA-I. The radioactive content of the media and cells was measured separately by scintillation counting. Sterol transfer was expressed as the

percentage of the radioactivity released from the cells into the media relative to the total radioactivity in the cells plus media. Values are mean \pm S.D. of ≥ 3 independent experiments.

Roles of individually amino acid residues in the conserved sequence

Next, we determined the roles of individual amino acid residues in the conserved sequence in ABCG1-mediated cholesterol efflux by substituting Asn316, Pro317, Asp319 and Phe320 with Ala individually. These ABCG1 mutants were transiently expressed in HEK293 cells. Their protein levels were comparable to that of the wild type protein (Figure 4A). As shown in Figure 4B, mutations P317A and D319A had no significant effect on ABCG1-mediated cholesterol efflux. On the other hand, the cells expressing mutant N316A or F320A showed a significant reduction in cholesterol efflux onto lipidated apoA-I when compared with cells expressing wild type ABCG1.

To further define how Asn316 and Phe320 affected ABCG1-mediated cholesterol efflux, N316 was mutated to Asp (N316Q) and Gln (N316D), and F320 was mutated to Ile (F320I) and Tyr (F320Y). Asp and Gln are more structurally similar to Asn, but Gln has an extra methylene group, and Asp is an acidic amino acid and has a carboxyl group instead of a carboxamine in Asn. Tyr is more structurally similar to Phe but has an extra hydroxyl group. Ile does not have an aromatic ring but is a hydrophobic amino acid residue like Phe. We also made a double mutation N316AF320A, in which both Asn 316 and Phe 320 were mutated to Ala, and a catalytic dead mutation K120M, in which the conserved lysine residue located at position 120 in the Walker A motif of the NBD of ABCG1 was mutated to methionine (K120M). Previously, it has been reported that this mutation essentially eliminates ABCG1-mediated cholesterol efflux (Gao et al., 2012; Kobayashi et al., 2006). We observed that all mutant proteins were

expressed at the similar levels to wild type ABCG1 when transiently expressed in HEK293 cells (Figure 4C). Mutations N316Q, N316D, like mutation K120M, significantly eliminated the ability of ABCG1 to mediate cholesterol efflux. Similarly, replacement of F320 with Ile reduced ABCG1-mediated cholesterol efflux. Mutation F320Y did not significantly impair ABCG1 function (Figure 4D).

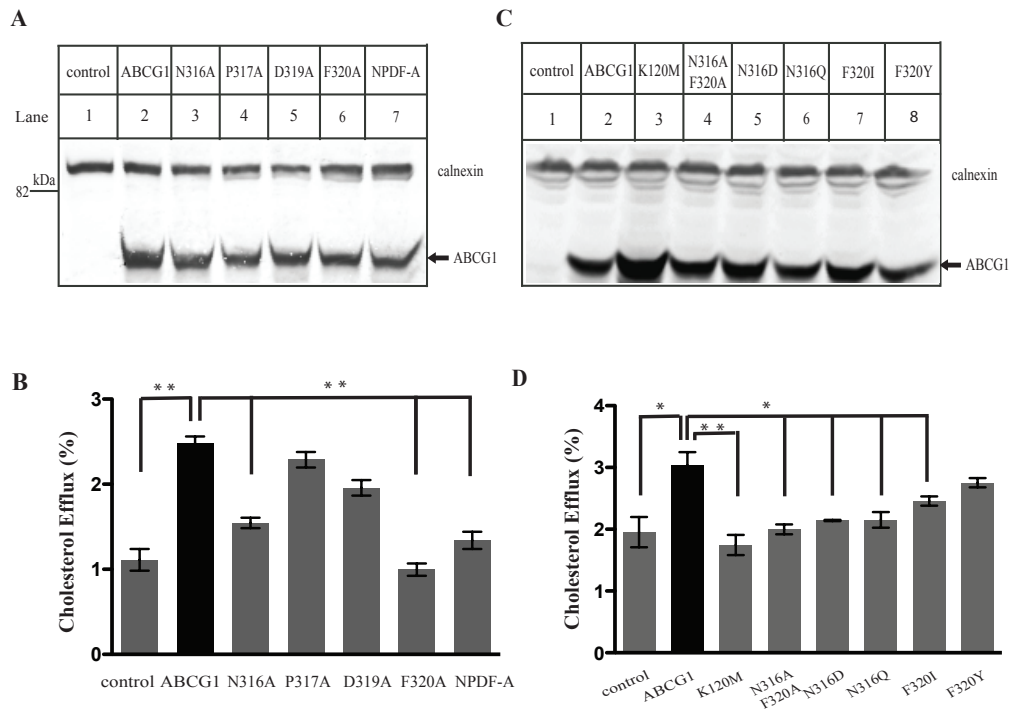


Figure 4. Role of individual residues within the conserved sequence in ABCG1-mediated cholesterol efflux.

Panels A and C: Expression of wild type and mutant ABCG1 in HEK293 cells transiently overexpressing wild type and mutant ABCG1 was determined as described in Figure 3C. ABCG1 was detected with a polyclonal anti-ABCG1 antibody, 4497. Calnexin was detected with a mouse monoclonal anti-calnexin antibody. Antibody binding was detected using IRDye-labeled goat anti-mouse or -rabbit IgG (Licor). The signals were detected by a Licor Odyssey Infrared Imaging System. Panel B and D: cholesterol efflux onto lipidated apoA-I was carried out as described in Figure 3D. *, $p < 0.05$; **, $p < 0.01$. Values are mean \pm S.D. of ≥ 3 independent experiments.

It has been reported that ABCG1 mediates oxysterol efflux (Terasaka et al., 2007). Thus, we investigated the ability of ABCG1 to mediate the efflux of 7-ketocholesterol, an abundant oxysterol in atherosclerotic lesions. We found that HEK 293 cells expressing wild type ABCG1 showed increased efflux of 7-ketocholesterol onto lipidated apoA-I when compared with the cells transfected with empty vector (Figure 5A). Next, we examined the effects of mutations of Asn316 and Phe320 on ABCG1-mediated 7-ketocholesterol efflux. As shown in Figure 5B, mutations N316A, N316Q, F320A and F320I all dramatically impaired the ability of ABCG1 to mediate 7-ketocholesterol efflux, while mutation F320Y remained similar to WT for the activity of 7-ketocholesterol efflux. These data were similar to what we observed in cholesterol efflux. Taken together, our findings provide evidence for the specific requirement of Asn at position 316 and Phe at position 320 for ABCG1-mediated cholesterol and oxysterol efflux.

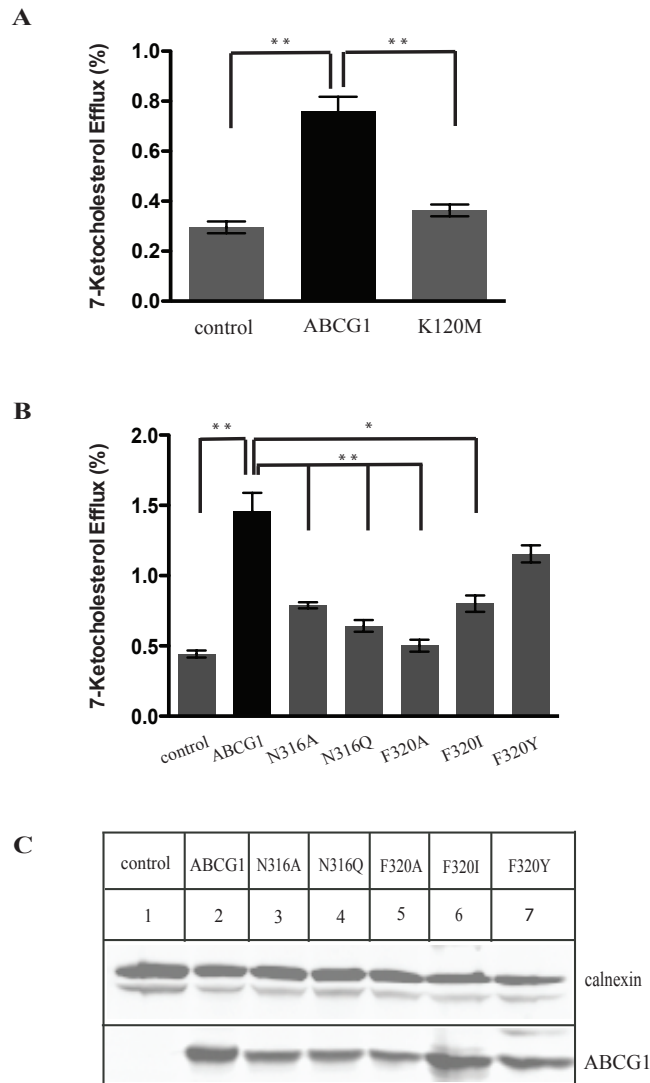


Figure 5. Effect of wild type and mutant ABCG1 on ABCG1-mediated 7-ketocholesterol efflux.

Panel A: HEK293 cells were transiently transfected with empty vector (control) or plasmid containing wild type (ABCG1) or mutant ABCG1 (K120M) cDNA and labeled with ^3H -7-ketocholesterol. After washing, the cells were incubated with lipidated apoA-I. The radioactive content of the media and cells was measured separately by scintillation counting. Sterol transfer was expressed as the

percentage of the radioactivity released from the cells into the media relative to the total radioactivity in the cells plus media. Panel B: Wild type and mutant ABCG1- mediated 7-ketocholesterol onto lipidated apoA-I. The experiment was carried out as described in panel A. *, $p < 0.05$; **, $p < 0.01$. Values are mean \pm S.D. of ≥ 3 independent experiments. Panel C: Expression of wild type and mutant ABCG1 in HEK293 cells stably expressing wild type and mutant ABCG1 was determined as described in Figure 3C. ABCG1 was detected with a polyclonal anti-ABCG1 antibody, 4497. Calnexin was detected with a mouse monoclonal anti-calnexin antibody. Antibody binding was detected using IRDye-labeled goat anti-mouse or -rabbit IgG (Licor). The signal was detected by a Licor Odyssey Infrared Imaging System.

Effect of mutations of Asn316 and Phe320 on the dimerization of ABCG1

Next, we investigated how mutations at positions 316 and 320 affected ABCG1 function. ABCG1 is a half transporter and functions as a homodimer (Kobayashi et al., 2006). Thus, we studied whether the mutations of Asn316 and Phe 320 had any effect on ABCG1 dimerization. Co-expression of half ABC transporters with two different tags followed by immunoprecipitation is a common technique to determine ABCG transporter dimerization (Gelissen et al., 2006; Graf et al., 2003; Kobayashi et al., 2006). We employed the same technique to explore the dimerization of mutant ABCG1 using ABCG1 with a C-Myc or HA tag at its COOH-terminus (ABCG1-Myc and ABCG1-HA). Cells were transiently transfected with a combination of wild type ABCG1-Myc and wild type ABCG1-HA. When we immunoprecipitated wild type ABCG1-Myc from the whole cell lysates, ABCG1-HA was co-immunoprecipitated with ABCG1-Myc in the cotransfected cells (Figure 6, lane 6). Thus ABCG1 forms homodimers, consistent with previous findings (Gelissen et al., 2006; Kobayashi et al., 2006). Similar experiments were performed on cells cotransfected with C-Myc- and HA-tagged mutant N316Q or F320I. As shown in Figure 6 (lanes 7, 8), N316Q-HA and F320I-HA were efficiently co-precipitated with N316Q-Myc and F320I-Myc, respectively. Therefore, mutations N316Q and F320I did not significantly affected ABCG1 dimerization. To confirm the results, we performed Gel filtration chromatography (Figure 7). HEK293 cells stably expressing wild type ABCG1 or mutants were lysed and applied to a Superose-12 column. The majority of wild type ABCG1 was eluted at molecular weight around 670 kDa, which is much

higher than the apparent molecular weight of an ABCG1 dimer (~150 kDa). It is possible that ABCG1, like ABCG2 (Xu et al., 2004), forms a self-oligomer, or associates with other proteins to form a protein complex. As shown in Figure 7, the gel filtration patterns of N320D and F320I were similar to that of wild type ABCG1, indicating that mutations at Asn316 and Phe320 do not affect the formation of the high molecular weight protein complex of ABCG1.

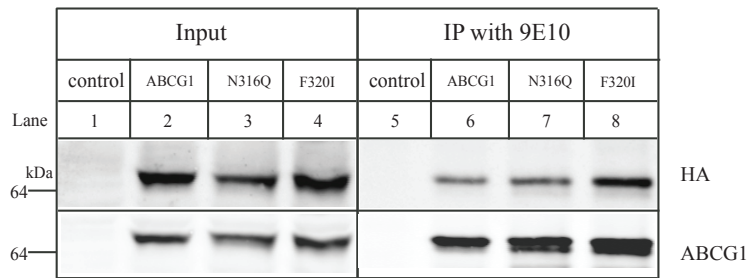


Figure 6. Effects of mutations of N316D and F320I on ABCG1 dimerization.

HEK293 cells were transiently transfected with a combination of wild type or mutant ABCG1-Myc and ABCG1-HA. The whole cell lysates and immunoprecipitated protein eluted from 9E10 (anti C-Myc antibody) -conjugated beads were fractionated by 8% SDS-PAGE and immunoblotted with anti-HA antibody and anti-ABCG1 antibody, 4497.

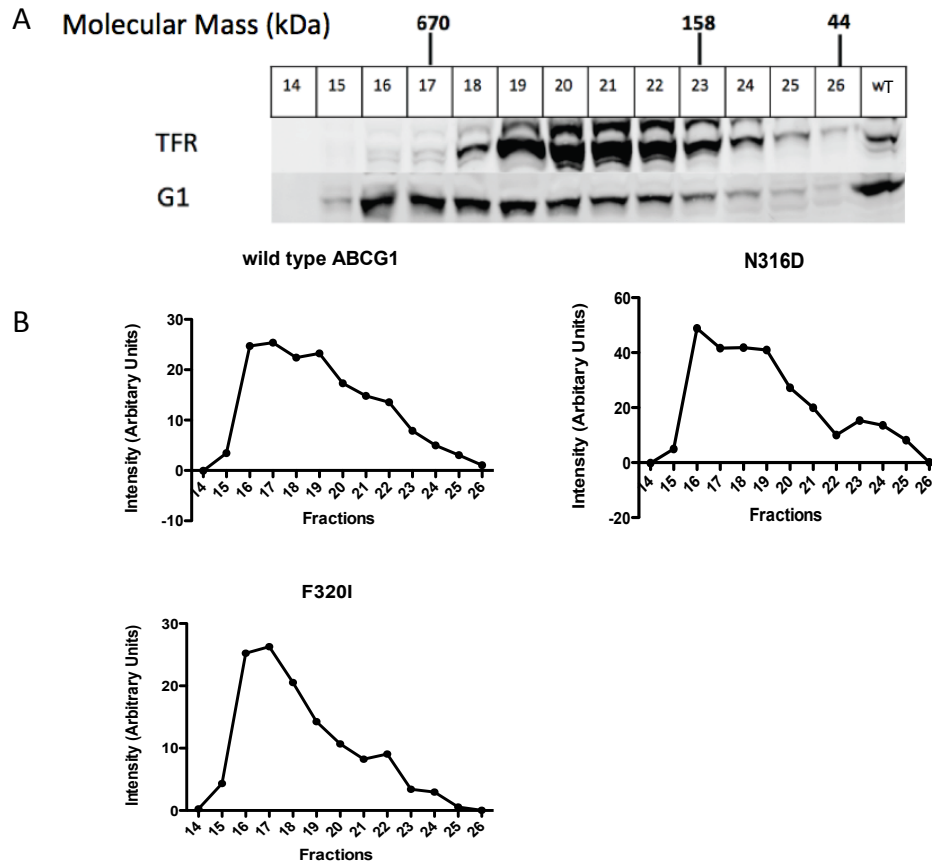


Figure 7. Gel filtration chromatography of wild type and mutant ABCG1.

Gel filtration of wild type and mutant ABCG1. HEK293 cells stably expressing wild type or mutant ABCG1 were solubilized in 500 μ l of lysis buffer B and centrifuged for 20 min at 20,817 rcf at 4°C to remove insoluble materials. The supernatant was loaded onto a Superose-12 10/300 GL column equilibrated with the lysis buffer B. The elution was collected at 0.5 ml per fraction and precipitated with TCA overnight at 4°C. The pellets were washed with acetone and dried. The dried pellets were dissolved in 9 M urea and subjected to SDS-PAGE and immunoblotting. The retention time of ABCG1 was determined by SDS/PAGE

and immunoblotting of the collected fractions. Panels A: gel filtration fractions were blotted with a polyclonal anti-ABCG1 and a monoclonal anti-Tfr antibody, respectively. The elution positions of the following protein standards are shown: ferritin (670 kDa), aldolase (158 kDa), and ovalbumin (44 kDa). Similar results were obtained in two independent experiments. Panel B: Densitometry of wild type ABCG1 and mutants N316D and F320I in each fraction. The proteins were quantified by measuring the intensity of the Western blot using a Licor software and plotted against fraction numbers.

Effects of mutations on ABCG1 trafficking

ABCG1-mediated cholesterol efflux mainly occurs at the cell surface, where the transporter delivers cholesterol to cell-surface pools that can be picked up by lipidated lipoproteins (Vaughan and Oram, 2005). Others and we have shown that ABCG1 localizes to the plasma membrane (Gao et al., 2012; Kobayashi et al., 2006; Vaughan and Oram, 2005; Wang et al., 2006a; Xie et al., 2006). Thus, we investigated whether mutations at positions 316 and 320 influenced the trafficking of ABCG1 to the plasma membrane using cell surface biotinylation experiments. Plasma membrane proteins in the cells stably expressing wild type or mutant ABCG1 were biotinylated by sulfo-NHS-biotin at 4°C and precipitated using NeutrAvidin beads, followed by immunoblotting with an anti-ABCG1 antibody, 4497. As shown in Figure 8B, we could detect wild type ABCG1 but not calnexin in the cell surface, biotinylation part (lane 2), suggesting that ABCG1 traffics to the plasma membrane, consistent with previous reports (Gao et al., 2012; Vaughan and Oram, 2005). Mutants NPDF-A, N316AF320A, N316D, N316Q and F320I all showed much less cell surface ABCG1 when compared to the wild type protein (Figure 8B, lanes 3 to 7), although they had similar total proteins in the whole cell lysates (Figure 8A). On the other hand, replacement of Phe320 with another aromatic amino acid Tyr did not cause any reduction in the cell surface expression of ABCG1 (lane 8). Thus, mutations of Asn316 and Phe320 except for F320Y affect the trafficking of ABCG1 to the cell surface.

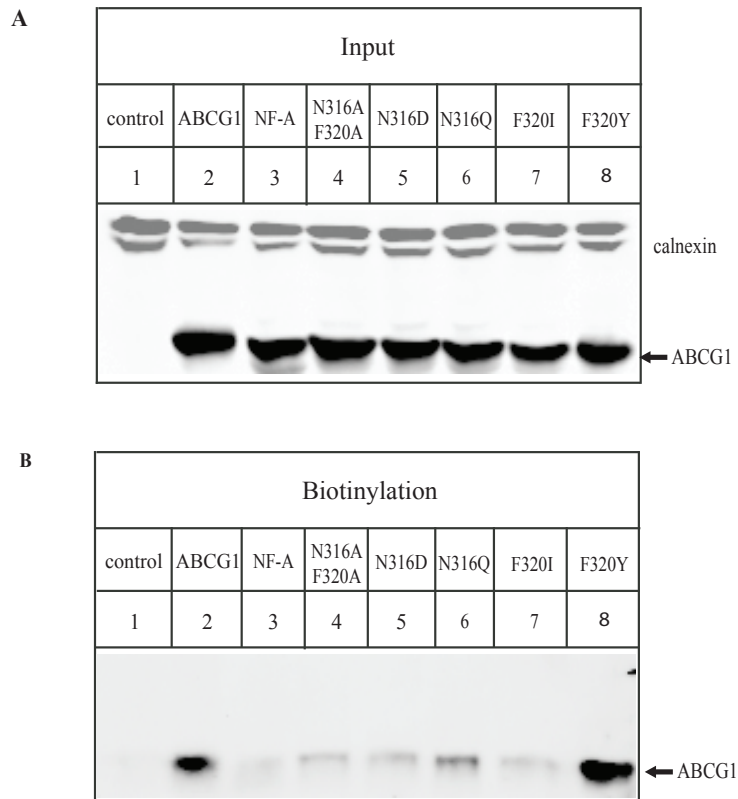


Figure 8. Trafficking of wild type and mutant ABCG1 in HEK293 cells.

HEK293 cells transiently expressing WT or mutant ABCG1 were biotinylated exactly as described. Biotinylated proteins from the cell surface (Biotinylation) and proteins from the whole cell lysate (Input) were analyzed by SDS/PAGE (8%) and immunoblotting. ABCG1 was detected using a polyclonal anti-ABCG1 antibody and calnexin was detected with a polyclonal antibody.

To further confirm the finding and determine the subcellular localization of these mutations, we performed confocal microscopy on HEK 293 cells stably expressing wild type and mutant ABCG1. Cell nuclei were detected by DAPI and shown as blue. ABCG1 was detected with a polyclonal anti-ABCG1 antibody, H-65, and shown as green (Figure 9, left panel). The cellular organelle markers including the plasma membrane marker, Na⁺/K⁺-ATPase, and the endoplasmic reticulum (ER) marker, calnexin were detected by their specific monoclonal antibodies and shown as red. No ABCG1 signal was detected in mock-transfected HEK293 cells. As shown in Figure 9, significant amount of wild type ABCG1 could be detected on the cell periphery (top, left), which was co-localized with the plasma membrane marker, Na⁺/K⁺-ATPase and shown as yellow (top, right). The subcellular distribution of N316D and F320I were significantly different from that of the wild type protein. In the overlap panel (right), both N316D and F320I were not co-localized with Na⁺/K⁺-ATPase (right panel). To further define the subcellular localization of mutant ABCG1, we next incubated the cells with an anti-calnexin antibody, and observed that there were significant amount of N316D and F320I co-localized with the ER marker (Figure 9). Similar experiments were performed on cells stably expressing mutations N316D and F320Y. The subcellular distribution of N316Q was same as that of N316D and F320I, whereas F320Y showed a similar distribution pattern as wild type ABCG1. Taken together, our data clearly showed that mutations of Asn326 and Phe320 except for F320Y affect the trafficking of ABCG1.

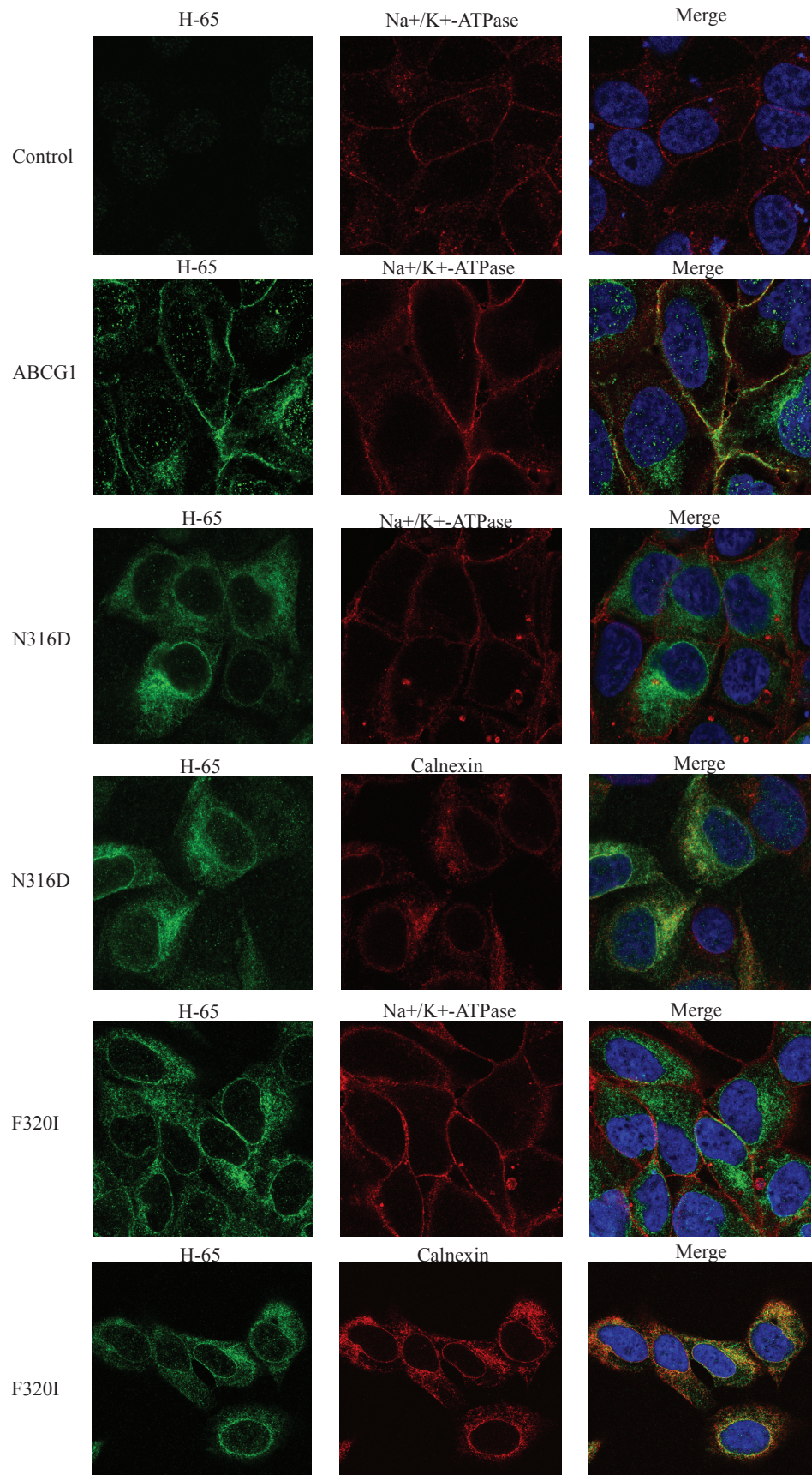


Figure 9. Immunofluorescence localization of ABCG1 in stably transfected HEK 293 cells.

The subcellular localization of wild type and mutant ABCG1 was determined by confocal microscopy as described. ABCG1 was detected using a polyclonal anti-ABCG1 antibody (H-65). Location of ABCG1 is indicated in green. Nuclei were stained with DAPI and shown in blue. The ER marker, calnexin, and the plasma membrane marker, Na⁺K⁺-ATPase, were detected using their specific monoclonal antibodies and shown in red. Transfectants that expressed either wild type or mutant ABCG1 were indicated in the figure. An x-y optical section of the cells illustrates the distribution of the wild type and mutant proteins between the plasma and intracellular membranes.

Effect of mutations on the ATPase activity of ABCG1

To examine the ATPase activity of mutant ABCG1, a baculovirus expression system was used to produce both wild type and mutant forms of ABCG1 in insect sf9 cells. A mutant ABCG1, in which the highly conserved lysine in the Walker A motif was replaced with Met, was used as a negative control. In all ABC proteins studied, this Lys residue is essential for ATP binding and hydrolysis (Cserepes et al., 2004). Inside-out membrane vesicles were prepared from insect sf9 cells expressing WT or mutant ABCG1 using nitrogen cavitation (Gao et al., 1996) and used to examine ATPase activity in the presence of 10 mM ATP with or without an ATPase inhibitor beryllium fluoride (BeFx). Beryllium fluoride, a phosphate analog, can efficiently inhibit ATP hydrolysis by ABC transporters (Wang et al., 2006b). The release of Pi from ATP by ATPases was measured by the absorbance at 650 nm and converted into phosphate concentration based on the phosphate standard curve. The BeFx sensitive ATPase activity was calculated by subtracting the ATPase activity in the presence of BeFx from the ATPase activity in the absence of BeFx. The BeFx sensitive ATPase activity of K120M was used as background since the mutant has no ATPase activity. The ATPase activity of wild type ABCG1 and mutants was calculated by subtracting the BeFx sensitive ATPase activity of K120M from the measured ATPase activity and then normalized to total ABCG1 protein level. As shown in the Figure 10, N316Q and F320I significantly reduced the ATPase activity of ABCG1.

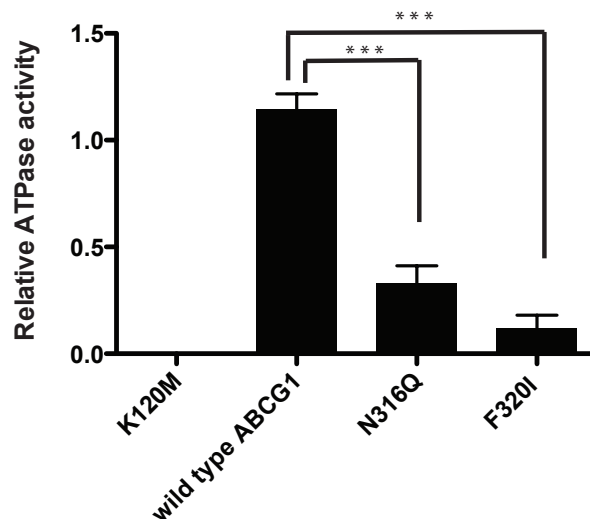
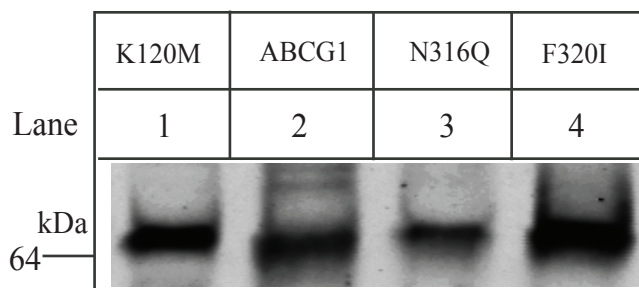


Figure 10. ATPase activity of ABCG1 in sf9 cell membrane vesicle.

The ATPase activities of WT or mutant ABCG1 in sf9 cell membrane vesicles were measured as description (see Chapter 2). Upper panel: The expression levels of wild type and mutant ABCG1 in membrane vesicles used for ATPase assay were determined by SDS/PAGE (8%) and immunoblotting. ABCG1 was detected using a polyclonal anti-ABCG1 antibody, 4497. Bottom panel: ATP hydrolysis was assayed for 1h at 37 °C and the amount of inorganic phosphate was determined as described in Experimental Procedures and normalized to total ABCG1 protein level. ***, $p < 0.0001$.

Effect of mutation on the stability of ABCG1

Next, we performed a pulse-chase experiment to determine the effect of the mutations on ABCG1 stability. HEK 293 cells stably expressing wild type or mutant N316Q and F320I were metabolically labeled with [³⁵S]-Met/Cys and then chased with excess Met/Cys for the indicated time periods. Immunoprecipitated ABCG1 was subjected to immunoblotting for detection of ABCG1 protein levels and to X-ray film exposure for detection of ³⁵S signal, respectively. The total protein levels were varied over the 4 h time course. Thus, the densitometry of ³⁵S signal bands was normalized by the densitometry of total protein signal bands (Figure 11). At 1 h time point, the ³⁵S labeling of wild type and N316Q was reduced to approximately 50% when compared to the 0 time point, while the ³⁵S labeling of F320I was reduced to approximately 40%. At 4h, the ³⁵S labeling of both mutation N316Q and F320I was reduced to less than 10%, while the ³⁵S labeling of wild type protein was reduced to around 20%. Thus, the mutations of Asn and Phe in ABCG1 appear not to have significant effect on ABCG1 stability.

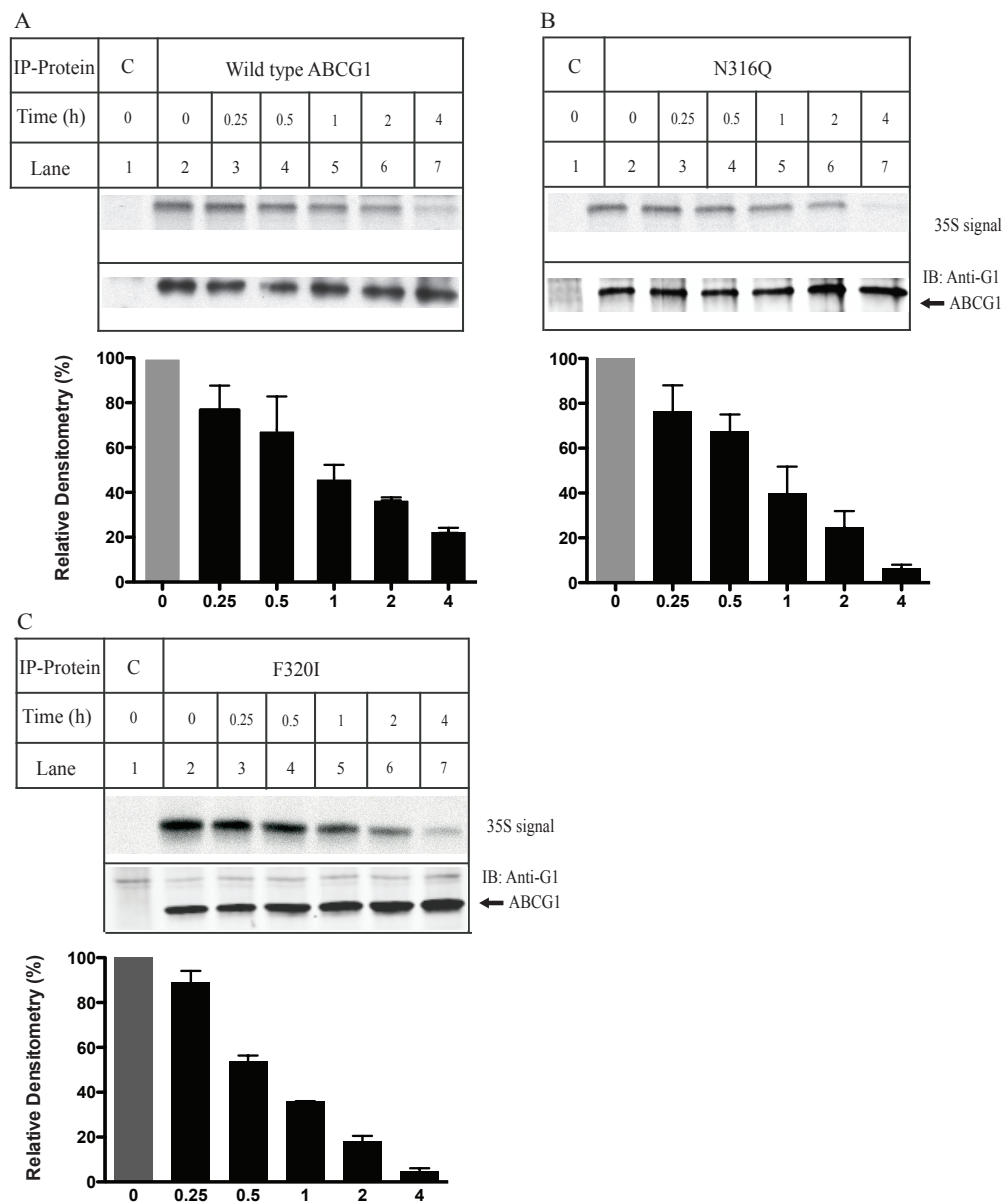


Figure 11. Metabolic labeling of cells with ^{35}S Cys/Met.

Top figures in each panel: HEK293 cells stably expressing wild type ABCG1 or mutant N316Q or F320I were metabolically labeled with [^{35}S]-Met/Cys (100 $\mu\text{Ci/ml}$) as described. The whole cell lysates were made and same amount of total proteins was incubated with 4497 (anti ABCG1 antibody)-beads.

Immunoprecipitated ABCG1 was eluted and subjected to SDS-PAGE (8%). ABCG1 protein was detected by immunoblotting with a polyclonal anti-ABCG1 antibody, 4497. ³⁵S signal was detected by X-ray film exposure. Similar results were obtained from two more independent experiments. Bottom figures in each panel: Relative densitometry. The relative signal intensities were determined by densitometry using Image J Analysis Software. The relative densitometry was the ratio of the densitometry of ABCG1 ³⁵S signal normalized to total protein signal at different time points to that of ABCG1 at time 0. Values are mean ± S.D. of 3 independent experiments. The relative densitometry of ABCG1 at time 0 was defined as 100%.

Discussion

In the present study, we identified a highly conserved sequence present in all five ABCG transporter family members. The sequence is located between the NBD and the transmembrane domain and contains five amino acid residues, Asn, Pro, Ala/Phe, Asp, and Phe. Two amino acid residues, Asn at position 316 and Phe at position 320 in ABCG1, played important roles in regulating ABCG1 function. Replacement of Asn316 with Ala, Gln or Asp essentially eliminated ABCG1-mediated sterol efflux. Substitution of Phe320 with Ala or Ile also significantly impaired ABCG1 function tested, but mutation of Phe320 to Tyr had no significant effect. We further demonstrated that mutations of Asn360 and Phe320 except for F320Y mainly colocalized with the ER marker, calnexin, whereas wild type protein mainly colocalized with the plasma membrane marker, Na⁺K⁺-ATPase.

How did these mutations affect ABCG1 trafficking? One simple explanation is that they may grossly disrupt ABCG1 structure and cause misfolding of the proteins. For instance, misfolded mutants of the human P-glycoprotein and CFTR are retained in the ER and rapidly degraded, resulting in lower protein levels (Cheng et al., 1990; Loo and Clarke, 1997). However, the protein levels of the ABCG1 mutants in transiently transfected and stable cells are comparable with that of wild type ABCG1 (Figure 4A, 4C and 8A). Furthermore, the pulse-chase experiment showed that the mutations had no significant effect on ABCG1 stability and mutant proteins formed homodimers and protein complexes as efficiently as the wild type protein (Figure 6 and 7). In addition, since lack of

high-resolution structures of ABCG1 or related ABCG transporters, we used several secondary structure algorithms to predict the structure of the linker region between NBD and transmembrane domain in ABCG1 that contains the conserved sequence in the middle. Asn316 is predicted to be a random coil. Replacement of Asn with Ala, Gln or Asp is also predicted to be a random coil. On the other hand, Phe320 is predicted to form an alpha-helix by three secondary structure prediction methods or an extend strand by two algorithms. Replacement of Phe320 with Ile or Tyr does not change the predicted secondary structure. Taken together, these findings suggest that mutations of Asn316 and Phe320 might not result in a major perturbation of the structure of the protein.

Our findings revealed a specific requirement of Asn at position 316 in ABCG1. Replacement of Asn with a structurally similar amino acid residue, Gln, which has an extra methylene group behaves same as other mutations such as N316A and N316D, resulting in ER retention of ABCG1, virtually eliminating ABCG1-mediated cholesterol and 7-ketocholesterol efflux. All secondary structure prediction methods we used predict that there is an alpha helix or a beta strand starting from amino acid Asp319 to amino acid Ala325, which is near Asn316. The side chain of both Asn and Gln can form hydrogen bond interactions with the peptide backbone. However, Asn, but not Gln, can often function as “capping” the hydrogen bond interactions near the beginning and the end of alpha-helices, and in turn motifs in beta sheets, thereby stabilizing the secondary structure (Bell et al., 1992; Richardson and Richardson, 1988; Serrano et al., 1992). It is possible that mutation N316Q might cause subtle changes in the

secondary structure, affecting ABCG1 trafficking. However, despite the fact that Asp is a better helix-capping residue than Asn (Serrano et al., 1992), we observed that mutation of Asn316 to Asp, like N316Q, also impaired ABCG1 trafficking. Furthermore, all mutations of Asn316 are predicted to have no effect on the secondary structure in the region based on the secondary structure algorithms we used. Thus, it is unlikely that mutations at position 316 dramatically affect the local secondary structure of ABCG1. However, we cannot exclude the possibility that Asn may form hydrogen bond with the peptide backbone or other amino acid residues to stabilize the tertiary structure of the NH₂-terminus of ABCG1.

Mutation of Phe320 to Ala or Ile dramatically impaired ABCG1 trafficking and function. The secondary structure algorithms predict that mutation of Phe320 to Ala, Ile, or Phe has no effect on the secondary structure in the region. The side-chains of Phe and Tyr are involved in pairwise interactions not only in protein secondary structure and but also in tertiary and quaternary interactions (Serrano et al., 1991). Thus, it is possible that Asn316 and Phe320 are involved in stabilizing the ABCG1 NH₂-terminal tertiary structure through hydrogen bond formation and aromatic-aromatic interaction, respectively. This tertiary structure appears not to play an important role in protein stability and dimerization, but to be critical for ABCG1 trafficking out from the ER. A high resolution crystal structure of a ABCG transporter that is currently unavailable will give us detailed insights in how these two amino acid residues contribute to the stability of ABCG1 tertiary structure.

The mechanism underlying export of ABC transporters from the ER is

unclear. It has been reported that Sec24 of the COPII vesicular coat functions as a primary cargo selection subunit and plays an important role in selective export of membrane proteins from the ER. Sec24 has four isoforms in human cells and recognizes various ER export signals located in the cytoplasmic regions of transmembrane proteins such as di-phenylalanine (FF), di-tyrosine (YY), di-leucine (LL), di-isoleucine (II), di-valine (VV) and DxE (Farhan et al., 2007; Mancias and Goldberg, 2008; Sucic et al., 2011; Wendeler et al., 2007). The conserved sequence, NPADF, does not contain any consensus ER export motif, but it is near to several ER export signals present in the cytoplasmic NH₂-terminus of ABCG1. The di-Ile at positions 264 and 265 are completely conserved in ABCG family. Therefore, it is possible that both Asn316 and Phe320 are involved in stabilizing ABCG1 tertiary structure, which can facilitate possible interactions between Sec24 and the ER export signal present in ABCG1. It will be of interest to see if Sec24 is involved in ER export of ABCG1 and if mutations at Asn316 and Phe320 affect this process.

Most recently, it has been reported that ABCG1 localizes to intracellular endosomes (Tarling and Edwards, 2011). The author proposed that ABCG1 transfers sterols to the inner leaflet of the intracellular vesicles, and then these vesicles fuse with the plasma membrane and deliver cellular cholesterol to exogenous HDL. However, several lines of evidence showed that ABCG1 localizes to the cell plasma membrane. Vaughan *et al* utilized biotinylation approach to show that ABCG1 traffics to the cell surface when expressed in BHK cells (Vaughan and Oram, 2005). We used the same approach to reveal plasma

membrane localization of untagged ABCG1 in HEK293 cells (Gao et al., 2012). Xie *et al* reported that EGFP-tagged ABCG1, when transiently expressed in HeLa cells or THP-1 cells, appeared in the plasma membrane (Xie et al., 2006). Wang *et al* used confocal microscopy to show that ABCG1, when transiently expressed in HEK293 cells, localizes to the plasma membrane as well as intracellular organelles such as Golgi and endocytic recycling compartments (Wang et al., 2006a). Consistently, we found that ABCG1 in both transiently and stably transfected HEK293 cells co-localizes with the plasma membrane marker, Na⁺K⁺/ATPase. Thus, our findings provide more evidence for the cell surface localization of ABCG1. What accounts for the difference between our findings and data of Tarling et al (Tarling and Edwards, 2011) is unclear.

In summary, we found that replacement of Pro or Asp in the conserved sequence (NPA/FDF) in ABCG transporter subfamily with Ala had a significant effect on ABCG1-mediated cholesterol efflux. On the other hand, the first and last amino acid residues in the conserved sequence play an important role in ABCG1 trafficking and function.

Chapter 4 Identification the functional roles of a STAT3 binding sequence in ATP binding cassette transporter G1

Background

ABCG1 belongs to ABC superfamily, which is one of the largest protein families and contains ubiquitous integral membrane proteins present in all organisms. ABC transporters use the energy from ATP-binding and hydrolysis in the NBD of the transporters to mediate the efflux of a wide variety of substrates across the membrane bilayer. ABC transporters contain two TMDs that form the translocation pathway and two NBDs that hydrolyze ATP (Biemans-Oldehinkel et al., 2006). The TMDs have low sequence similarity among different transporters, while the NBDs are highly conserved, each consisting of a RecA-like subdomain containing Walker A and B motifs, and a helical subdomain containing the LSGGQ (Leu-Ser-Gly-Gly-Gln) signature motif. Most ABC proteins from eukaryotes encode full transporters, or half transporters that form a homo- or heterodimer. A full functional ABC transporter typically consists of two nucleotide-binding domains and two transmembrane domains. The transmembrane domains are mainly involved in substrate recognition, binding and transport, and the NBDs, which share a high degree of sequence and structural homology among different ABC transporters (Oswald et al., 2006), are responsible for the ATP binding and hydrolysis and consequently energize substrate transport. How the binding and hydrolysis of ATP leads to the transport

of a substrate across bilayer membranes is not fully understood. The X-ray crystallographic structures of several bacterial ABC transporters and most recently a eukaryotic full-length transporter ABCB1 (p-glycoprotein) reveal that the NBDs of ABC transporters are formed by association between the Walker A and Walker B motifs of one subunit and the signature motif of the other subunit. ATP binds at the interface between the two subunits to form a sandwich like structure. It is generally accepted that the transport cycle is initiated by substrate binding that gives rise to a conformational change in the transporter followed by sequential ATP binding to the NBDs and conformational change of the binding pocket, so that the substrate transfers from a high-affinity binding site to a low affinity binding site, enabling its release on the other side of the cellular membrane (Chang, 2007; Deeley et al., 2006; Rees et al., 2009; Seeger and van Veen, 2009). The transport cycle is completed by hydrolysis of ATP and subsequent energy transfer from the NBDs to the TMs, and by release of ADP and restoration of the “resting” high affinity state of the transporter (Chang, 2007; Higgins and Linton, 2004).

ABCG1 and ABCA1 function synergistically to efflux cellular free cholesterol onto exogenous acceptors and play pivotal roles in the initial and rate-limiting step of reverse cholesterol transport pathway (Gelissen et al., 2006; Vaughan and Oram, 2006). Recently, ABCA1 has been found to have anti-inflammatory functions, which represents another independent mechanism for protection against CVD besides mediating cholesterol efflux (Tang et al., 2009). Interaction between apoA-I and ABCA1 promotes cholesterol removal and also

other signaling molecules activation such as Janus kinase 2 (JAK2). Oram group found that ABCA1-mediated activation of JAK2 activates a transcription factor, STAT3 (Tang et al., 2009). STAT3 has an anti-inflammatory role in macrophages (Williams et al., 2007). There are two STAT3 binding sites present in ABCA1, which are necessary for the apoA-I/ABCA1/JAK2 activation of STAT3. Interaction of apoA-I with cholesterol-loaded macrophages reduces LPS-induced production of inflammatory cytokines tumor necrosis factor α , IL-1 β and IL-6. They propose a model of ABCA1/JAK2 dependent pathway for STAT3-mediated suppression of inflammatory cytokine production in macrophages: 1, ABCA1 forms cell-surface lipid domains enriched with phospholipids and free cholesterol; 2, apoA-I binds to ABCA1 and stimulates autophosphorylation of JAK2; 3, the activated JAK2 enhances the interaction of apoA-I with ABCA1 and creates STAT3 docking sites that promote JAK2-mediated phosphorylation of STAT3; 4, lipid-bound apoA-I is released from ABCA1-formed lipid enriched domain to generate nascent HDL particles, and phosphorylated STAT3 is translocated to the nucleus where it regulates transcription events to suppress production of inflammatory cytokines (Liu and Tang, 2012; Tang et al., 2009).

Human population studies have shown that plasma levels of HDL are inversely associated with the risk of cardiovascular diseases (Asztalos et al., 2005; Barter et al., 2007). The most investigated mechanism of HDL to prevent atherosclerosis is the reverse cholesterol transport process, in which accumulated cholesterol is transported by HDL from the vessel wall to the liver for the final excretion. Recently, HDL has been described to have various anti-inflammatory

properties (Patel et al., 2009), which may provide new insights into the prevention of atherosclerosis. The exact mechanisms for reducing inflammation by HDL, which usually presents as multifunctional lipoprotein complexes, however, are not fully understood. More interestingly, the anti-inflammatory role of HDL is more relevant with ABCG1 (Yvan-Charvet et al., 2010b).

Recently, several studies reported that loss of ABCG1 from macrophages results in multiple inflammatory effects. Baldan *et al* reported the progressive and chronic inflammatory process that accompanies the lipidosis in the lungs of *Abcg1*^{-/-} mice and claimed that cholesterol and/or cholesterol metabolites that accumulate in *Abcg1*^{-/-} lungs can trigger inflammatory signaling pathways (Baldan et al., 2008). Similarly, Wojcik *et al* found *Abcg1*^{-/-} macrophages have elevated pro-inflammatory cytokine production and increased apoptotic cell clearance. The authors proposed that ABCG1 deletion in macrophages causes a striking inflammatory phenotype and initiates onset of pulmonary lipidosis in mice (Wojcik et al., 2008).

We found that, like ABCA1, ABCG1 has one STAT3 binding site (YXXQ) in the N-terminal cytoplasmic region (Y157-I158-M159-Q160) (Figure 12). We therefore hypothesized that ABCG1 may also bind to STAT3 and act in an anti-inflammatory way. To test this hypothesis, we replaced Tyr157 and Gln160 with Ala to disrupt the STAT3 binding site. We could not detect co-immunoprecipitation between ABCG1 and STAT3. However, we found that mutation Y157A significantly reduced the efflux of cholesterol and 7-

ketocholesterol mediated by ABCG1, while mutation Q160A reduced ABCG1-mediated 7-ketocholesterol efflux without significant effect on cholesterol efflux.

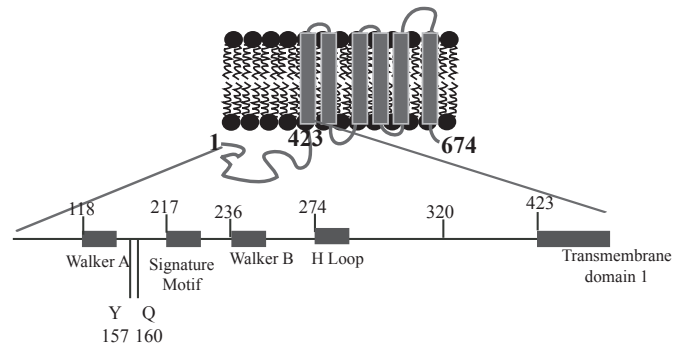


Figure 12. The predicted STAT3 binding site of ABCG1.

Predicted topology of ABCG1. The position of predicted STAT3 binding sequence (YXXQ) in NBD domain was shown.

Results

The association between STAT3 and ABCG1

We examined whether STAT3 and ABCG1 formed a molecular complex. Different detergents including Triton X-100, digitonin, and C12E9 were used to extract ABCG1 from HEK 293 cells stably expressing ABCG1. ABCG1 was immunoprecipitated from the whole cell lysates using 4497 conjugated beads. The eluted precipitated proteins were subjected to immunoblotting. The membranes were blotted with a polyclonal anti-ABCG1 antibody and a monoclonal anti-STAT3 antibody to detect ABCG1 and STAT3, respectively. As shown in Figure 13, we could not detect STAT3 in the immunoprecipitated samples.

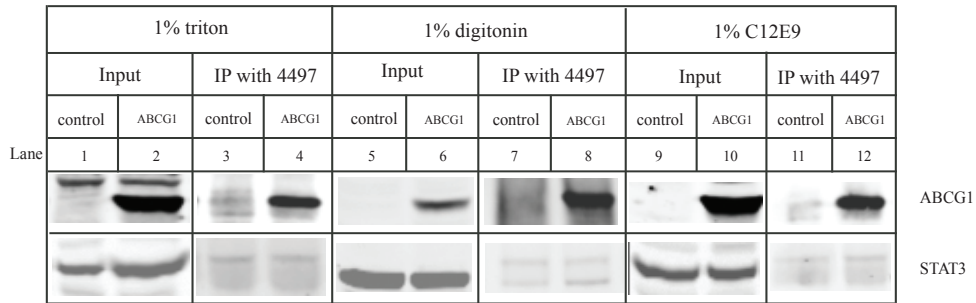


Figure 13. Immunoprecipitation of ABCG1.

HEK293 cells stably expressing ABCG1 were lysed in lysis buffer containing 1% Triton X-100, 1% digitonin or 1% C12E9. The whole cell lysates and immunoprecipitated protein eluted from 4497-conjugated beads were fractionated by 8% SDS-PAGE and immunoblotted with anti-STAT3 antibody and anti-ABCG1 antibody, 4497.

Effect of the STAT3 binding sequence on ABCG1 function

Next, we examined the potential roles of YXXQ sequence in ABCG1-mediated sterol efflux. Tyr 157 and Gln 160 were replaced with Ala. The efflux of cholesterol and 7-ketocholesterol was performed on HEK 293 cells transiently expressing wild type or mutant ABCG1. As shown in Figure 14, the expression levels of Y157A and Q160A were comparable to that of wild type protein. Y157A significantly reduced ABCG1-mediated efflux of both cholesterol and 7-ketocholesterol. On the other hand, Q160A dramatically impaired ABCG1-mediated 7-ketocholesterol efflux while having no significant effect on cholesterol efflux. Thus, Tyr 157 played an important role in ABCG1-mediated sterol efflux, while Gln 160 might be a determinant for the substrate specificity of ABCG1.

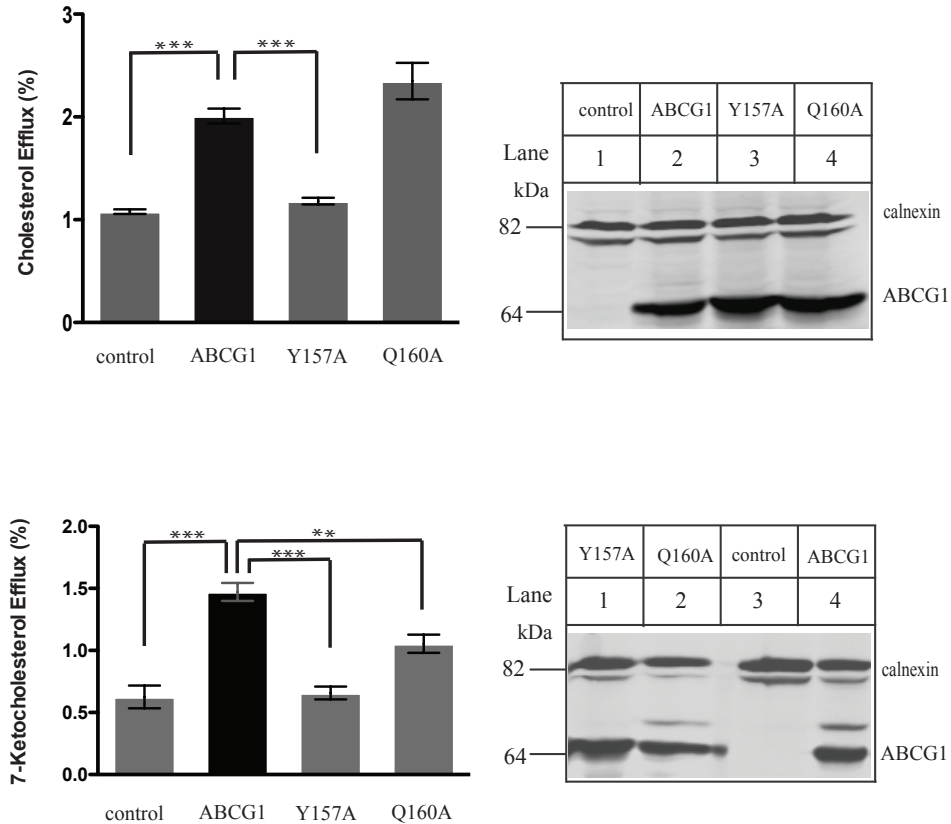


Figure 14. Effect of mutations on ABCG1-mediated sterol efflux.

Expression of wild type and mutant ABCG1 in HEK293 cells transiently overexpressing wild type and mutant ABCG1 was determined as described. ABCG1 was detected with a polyclonal anti-ABCG1 antibody, 4497. Calnexin was detected with a mouse monoclonal anti-calnexin antibody. Antibody binding was detected using IRDye-labeled goat anti-mouse or -rabbit IgG (Licor). The signals were detected by a Licor Odyssey Infrared Imaging System. Cholesterol and 7-ketocholesterol efflux onto lipidated apoA-I was carried out as described in Figure 3D. **, $p < 0.01$; ***, $p < 0.001$. Values are mean \pm S.D. of ≥ 3 independent experiments.

Effect of Y157A and Q160A on the dimerization of ABCG1

We then explored how mutations Y157A and Q160A affected ABCG1 function. ABCG1 forms a homodimer to be a functional transporter. We studied whether mutations Y157A and Q160A had any effect on ABCG1 dimerization. HEK 293 cells were transiently transfected with a combination of C-Myc- and HA- tagged wild type ABCG1, Y157A or Q160A. Myc-tagged proteins were immunoprecipitated from the whole cell lysates and subjected to SDS-PAGE and immunoblotting. The membranes were blotted with an anti-HA antibody to detect HA-tagged proteins. As shown in Figure 15, Y157A-Myc and Q160A-Myc were efficiently immunoprecipitated from the whole cell lysates. The levels of HA-tagged Y157A and Q160A in the immunoprecipitated pellets were comparable to that of wild type HA-tagged ABCG1. Therefore, mutations Y157A and Q160A did not affect ABCG1 dimerization.

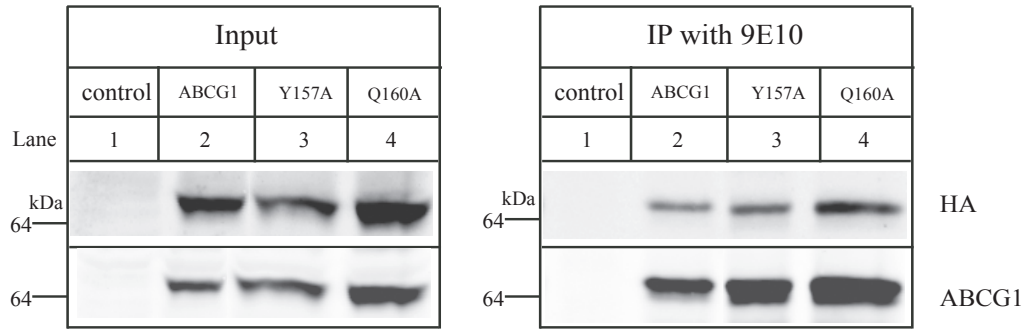


Figure 15. Effects of mutations of Y157A and Q160A on ABCG1 dimerization.

HEK293 cells were transiently transfected with a combination of WT or mutant ABCG1-Myc and ABCG1-HA. The whole cell lysates were subjected to 9E10-conjugated beads to immunoprecipitate Myc-tagged ABCG1. The immunoprecipitated proteins were eluted from 9E10-conjugated beads and fractionated by 8% SDS-PAGE, followed by immunoblotting with an anti-HA antibody to detect HA-tagged ABCG1 (top panel) or with an anti-ABCG1 antibody, 4497, to detect total Myc-tagged and HA-tagged ABCG1 (bottom panel).

Effects of Y157A and Q160A on ABCG1 trafficking

Next, we determined whether the mutations Y157A and Q160A affected the trafficking of ABCG1 to the cell surface using biotinylation. HEK 293 cells stably expressing WT or mutant ABCG1 were labeled with sulfo-NHS-biotin, and the whole cell lysates were applied to NeutrAvidin beads to precipitate labeled cell surface proteins. The biotinylated cell surface proteins were applied to SDS-PAGE and immunoblotted with anti-ABCG1 antibody, 4497. As shown in Figure 16, the levels of total protein and cell surface expression of mutations Y157A and Q160A were comparable to that of wild type protein (Figure 16 lanes 6, 7 and 8). To confirm the results, we performed confocal microscopy on HEK 293 cells stably expressing mutations Y157A and Q160A. Cell nuclei were detected by DAPI and shown as blue. ABCG1 was detected with anti-ABCG1 antibody, H-65, and shown as green. The plasma membrane marker, Na⁺/K⁺-ATPase was detected by a monoclonal anti- Na⁺/K⁺-ATPase antibody and shown as red (Figure 17). Similar to wild type ABCG1, mutations of Y157A and Q160A efficiently reached to the cell surface and co-localized with the plasma marker Na⁺/K⁺-ATPase (yellow). Therefore, mutations Y157A and Q160A did not affect trafficking of ABCG1 to the cell surface.

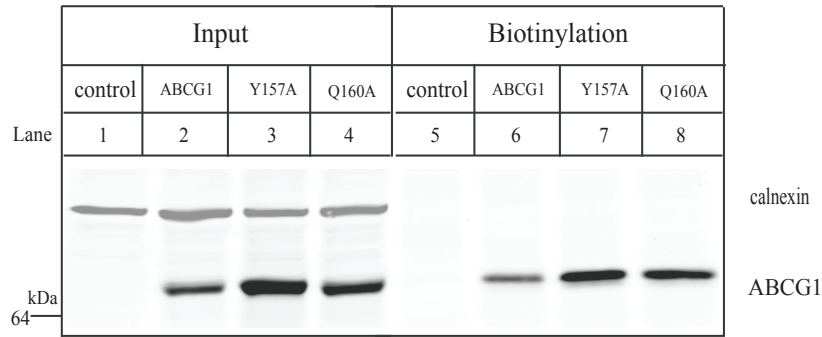


Figure 16. Biotinylation of Y157A and Q160A in HEK293 cells.

HEK293 cells transiently expressing WT, Y157A or Q160A were biotinylated as described in the legend to Figure 8. Biotinylated proteins from the cell surface (Biotinylation) and proteins from the whole cell lysate (Input) were analyzed by SDS/PAGE (8%) and immunoblotting. ABCG1 was detected using a polyclonal anti-ABCG1 antibody 4497 and calnexin was detected with a polyclonal antibody.

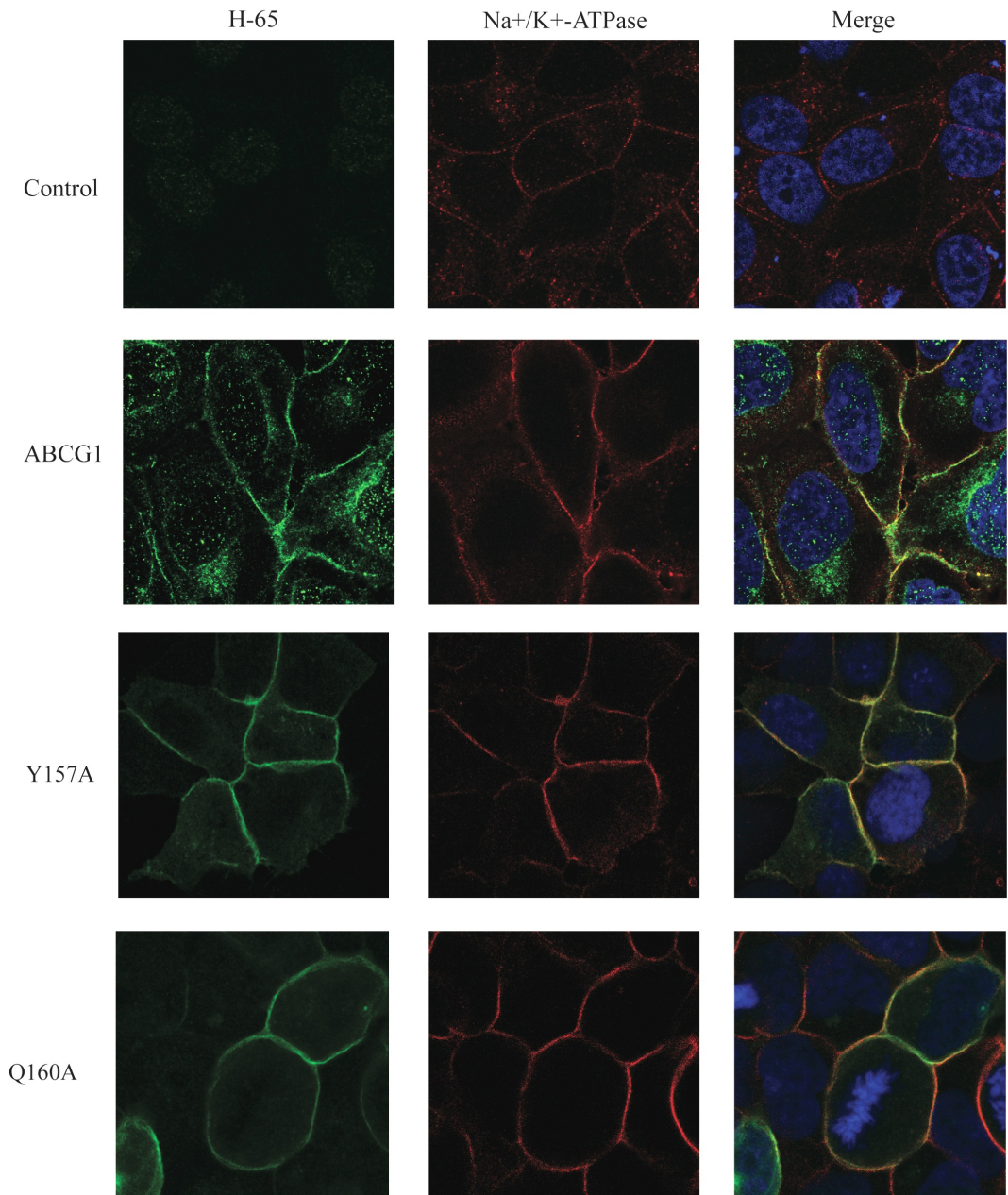


Figure 17. Immunofluorescence localization of wild type and mutant ABCG1 in stably transfected HEK 293 cells.

The subcellular localization of mutant Y157A and Q160A was determined by confocal microscopy as described in the legend to Figure 9. ABCG1 was detected

using a polyclonal anti-ABCG1 antibody (H-65). Location of ABCG1 mutant is indicated in green. Nuclei were stained with DAPI and are shown in blue. The plasma membrane marker, Na⁺K⁺-ATPase, was detected using its specific monoclonal antibody and are shown in red. An x-y optical section of the cells illustrates the distribution of the mutant proteins between the plasma and intracellular membranes.

Effect of Y157A and Q160A on the stability of ABCG1

The WT and mutant ABCG1 showed similar amount of total and cell surface protein levels, indicating that the two mutations might have no significant effect on ABCG1 stability. To further confirm this finding, we performed a pulse-chase experiment to determine the stability of wild type and mutant ABCG1 protein. HEK 293 cells stably expressing Y157A and Q160A were metabolically labeled with [³⁵S]-Met/Cys and then chased with excess Met/Cys for the indicated time periods. Immunoprecipitated ABCG1 was subjected to immunoblotting for detection of ABCG1 protein levels and to X-ray film exposure for detection of ³⁵S signal, respectively. The protein stability was expressed as relative densitometry that is calculated by normalizing the densitometry of ³⁵S signal bands with that of the total protein signal bands. (Figure 18, low panel). The ³⁵S patterns were essentially the same among the wild type and mutant proteins. At 4 h, the ³⁵S labeling of mutants and wild type ABCG1 (Figure 11, panel A) was reduced to about 20%. Therefore, mutations Y157A and Q160A had no significant effect on ABCG1 stability.

Effect of Y157A and Q160A on ATPase activity of ABCG1

Given that both Tyr157 and Gln160 are located in the NBD of ABCG1, we tested whether the mutations affected ATPase activity of ABCG1. Inside-out membrane vesicles were prepared from sf9 cells expressing WT or mutant ABCG1 and the ATPase activity was measure as described. The ATPase activity of wild type ABCG1 and mutants were calculated by subtracting the BeFx

sensitive ATPase activity of K120M that was used as a control for the measured ATPase activity. As shown in Figure 19, the BeFx sensitive ATPase activity of both Y157A and Q160A was comparable to that of the wild type protein. Thus, Y157A and Q160A had no detectable effect on the ATPase activity of ABCG1.

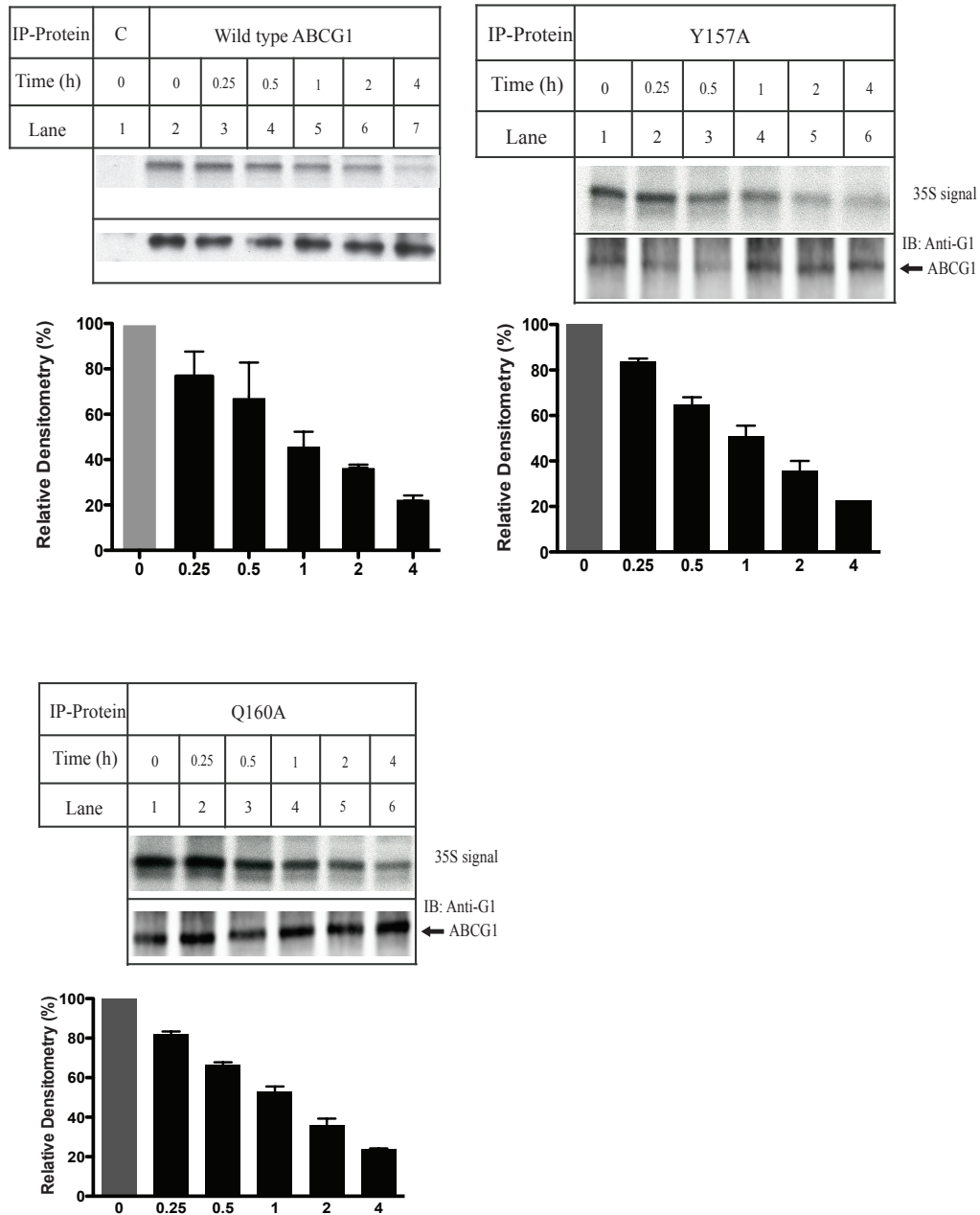


Figure 18. Metabolic labeling of cells with ^{35}S Cys/Met.

Upper figure in each panel: HEK293 cells stably expressing wild type ABCG1, mutant Y157A or Q160A were metabolically labeled with [^{35}S]-Met/Cys (100 $\mu\text{Ci/ml}$) as described in chapter 2. The whole cell lysates were made and same amount of total proteins were incubated with 4497-beads.

Immunoprecipitated ABCG1 was eluted and subjected to SDS-PAGE (8%). ABCG1 protein was detected by immunoblotting with a polyclonal anti-ABCG1 antibody, 4497. ^{35}S signal was detected by X-ray film exposure. Similar results were obtained from two more independent experiments. Bottom parts of panels: Relative densitometry. The relative signal intensities were determined by densitometry using Image J Analysis Software. The relative densitometry was the ratio of the densitometry of ABCG1 ^{35}S signal normalized to total protein signal at different time points to the densitometry of ABCG1 at time 0. Values are mean \pm S.D. of 3 independent experiments. The relative densitometry of ABCG1 at time 0 was defined as 100%.

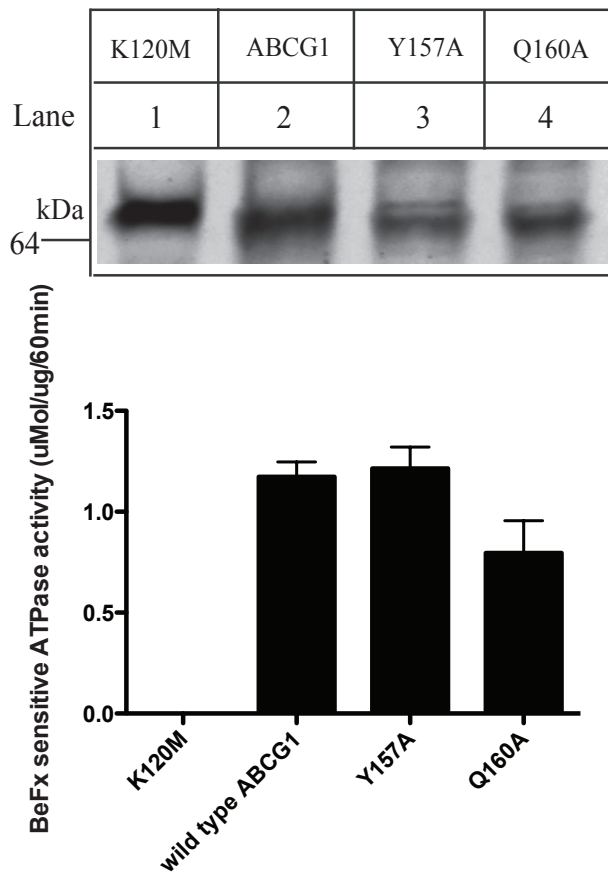


Figure 19. ATPase activity of ABCG1 in sf9 cell membrane vesicle.

The ATPase activities of wild type or mutant ABCG1 in sf9 cell membrane vesicles were measured as described (see Chapter 2). Upper panel: The expression levels of wild type and mutant ABCG1 were determined by SDS/PAGE (8%) and immunoblotting. ABCG1 was detected using a polyclonal anti-ABCG1 antibody, 4497. Bottom panel: ATP hydrolysis was assayed for 1 h at 37 °C and the amount of inorganic phosphate was determined as described in Experimental Procedures.

Discussion

In the present study, we demonstrated that Tyr157 and Gln160 in the STAT3 binding sequence of ABCG1 played an important role in ABCG1-mediated sterol efflux. Replacement of Tyr157 with Ala eliminated the efflux of both cholesterol and 7-ketocholesterol efflux mediated by ABCG1. Substitution of Gln160 with Ala had no effect on the cholesterol efflux but significantly impaired ABCG1 mediated 7-ketocholesterol efflux. Furthermore, we demonstrated that the mutations of Y157A and Q160A had no significant effect on the dimerization, trafficking, stability and ATPase activity of ABCG1.

We hypothesized that ABCG1 might associate with STAT3 and regulate inflammation through a similar mechanism as ABCA1. However, we could not detect an interaction between ABCG1 and STAT3 by co-immunoprecipitation. One simple explanation is that ABCG1 does not interact with STAT3 even though it contains a STAT3 binding motif and that ABCG1 and ABCA1 regulate inflammation through different mechanisms. For example, ABCG1 but not ABCA1 mediates 7-ketocholesterol efflux. 7-ketocholesterol is pro-inflammatory and induces inflammation *in vivo* (Amaral et al., 2013). Thus, it is possible that ABCG1-mediated 7-ketocholesterol efflux decreases cellular levels of this oxysterol and consequently reduces inflammation. Alternatively, the association between ABCG1 and STAT3 may be weak and transient, and cannot be detected by our co-immunoprecipitation assay. More studies such as co-immunoprecipitation in the presence of a chemical crosslinker are needed to address this question.

Studies of ABCA1 show that the integrity of the two STAT3 binding sites is not required for ABCA1-mediated cholesterol and phospholipid efflux. Mutations of the two STAT3 binding sites completely abolish the ability of ABCA1 to activate and bind STAT3 while having no effect on the cholesterol export function of ABCA1 (Tang et al., 2009). Here, we found that mutations of the consensus sequence in STAT3 binding site impaired ABCG1-mediated sterol efflux. ABCA1 mediates cholesterol and PC efflux simultaneously onto lipid-poor apoA-I (Smith et al., 2004). Several lines of evidence demonstrate that ABCA1 directly interacts with apoA-I (Chroni et al., 2004; Fitzgerald et al., 2004; Fitzgerald et al., 2002; Nieland et al., 2004; Wang et al., 2000). On the other hand, ABCG1 promotes efflux of cholesterol and oxysterols onto lipoproteins including HDL without binding lipoprotein particles (Wang et al., 2004; Wang et al., 2006a). Thus, the mechanisms of the two transporters-mediated sterol efflux are different and the STAT3 binding site in ABCG1 but not in ABCA1 regulates that ability of the transporter to mediate sterol efflux.

How do mutations Y157A and Q160A affect ABCG1-mediated sterol efflux, especially for mutation Q160A only impairs ABCG1-mediated 7-ketocholesterol efflux? Similar results were found in previous study on function analysis of ABCG5/ABCG8 (Zhang et al., 2006). Substitution of the conserved lysine in Walker A motif of ABCG5 to arginine abolishes ABCG5/G8-mediated transport of cholesterol but not plant sterol. Our studies showed that the two mutations had no detectable effect on ABCG1 dimerization, stability, trafficking and ATPase activity. Studies of other ABC transporters have shown that the

membrane spanning domains of typical ABC transporters that contain 6 transmembrane alpha-helices form the putative pathway for substrates across the lipid bilayer and are believed to contribute to substrate recognition and specificity for each transporter (Daoud et al., 2001; Karwatsky et al., 2005; Loo and Clarke, 2005, 2008; Zhang et al., 2001a; Zhang et al., 2003). Both Tyr157 and Gln160 are located in the N-terminal cytoplasmic region of ABCG1. Studies in MRP1/ABCC1 have shown that the cytoplasmic loop 7 may interact with transmembrane domains and NBD and then affects the substrate specificity of MRP1/ABCC1 (Koike et al., 2004; Letourneau et al., 2008). We have demonstrated that ABCG1 is palmitoylated at five cysteine residues located at positions 26, 150, 311, 390 and 402 in the N-terminal cytoplasmic region. Protein palmitoylation is a dynamic posttranslational protein modification that is the attachment of fatty acids, such as palmitic acid, to the side chain of cysteine residues in proteins. This reversible modification regulates the association of proteins with specific membranes (Baekkeskov and Kanaani; Charollais and Van Der Goot, 2009; Greaves et al., 2009). Thus, it is possible that the palmitoylation modification of ABCG1 may bring Tyr157 and Gln 160 close to the transmembrane domains of ABCG1. Consequently, the two residues contribute to substrate recognition and/or specificity of ABCG1 directly or indirectly.

In addition, Tyr 157 and Gln160 are located in the NBD of ABCG1. They are not on the three conserved motifs, the Walker A, Walker B and signature motif. However, Tyr is located between the Walker A motif and signature motif. Gln 160 is the most conserved residue Gln in the Q loop of ABC transporters. Q

loop is a conserved structural feature of all NBDs in ABC transporters and plays a central role in the function of ABC transporters (Chen et al., 2003; Diederichs et al., 2000; Gaudet and Wiley, 2001; Hung et al., 1998; Karpowich et al., 2001; Smith et al., 2002; Yuan et al., 2001). The crystallographic structures of NBDs of ABC transporters reveal that the Q loop positions to mediate the tight binding interaction between the TMD and NBD, it also reaches in toward the γ phosphate of ATP in the closed, ATP-bound conformation (Chen et al., 2003). In the present study, we found that mutations Y157A and Q160A had no significant effect on ATPase activity of ABCG1. However, we cannot rule out the possibility that the two mutations may cause subtle changes in NBD, which could not be detected by the ATPase assay used. ATP binding and trapping experiments may help answer this question and elucidate the exact role of the two residue in ATP binding and hydrolysis in NBD of ABCG1. Unfortunately, 8-azido [α - 32 P] ATP is not commercially available at this time.

In summary, we found that residue Tyr 157 played an important role in ABCG1-mediated efflux of cholesterol and 7-ketocholesterol, while Gln 160 somehow regulated the substrate specificity of ABCG1. Further studies are required to uncover the mechanisms by which the residues affect the function of ABCG1.

Chapter 5 General Conclusion and Discussion

Cholesterol is a key component of cell membranes, and cellular cholesterol levels are tightly regulated. Excessive cholesterol levels in macrophages trigger the foam cell formation and atherosclerosis initiation. ABCG1 is an important protein to regulate cholesterol content in many tissues and thus could be a therapeutic target for anti-atherosclerosis. However, the detailed mechanism of ABCG1-mediated sterol efflux is still uncovered yet.

In this thesis, we characterized the functional role of a highly conserved sequence NPA/FDF present between the NBD domain and TM domain of ABC subfamily G proteins. The first data we gathered showed that two residues Asn 316 and Phe 320 in the conserved motif played an important role in regulating ABCG1 function. Mutations on these two residues did not affect the dimerization and stability but affected the trafficking and ATPase activity of ABCG1. In the second part, we characterized the functional role of residues Tyr 157 and Gln 160 located in a STAT3 binding motif in the NBD domain of ABCG1. We found that Y157A impaired the ability of ABCG1 to mediate cholesterol and 7-ketocholesterol efflux. Q160A, on the other hand, abolished ABCG1-mediated efflux of 7-ketocholesterol but not cholesterol. Mutations Y157A and Q160A had no effect on the dimerization, trafficking, stability and ATPase activity of ABCG1. Our studies in this thesis provide more detailed biochemical evidence to understand how ABCG1 works. Moreover, the unexpected result we obtained was

that residue Gln 160 plays a role in substrate specificity of ABCG1 would help to understand the mechanism of ABCG1-mediated oxysterol efflux.

Oxysterols are oxygenated products of cholesterol that are important as intermediates or end products in cholesterol catabolic pathways. Their ability to cross cell membranes and the blood-brain barrier at a faster rate than cholesterol itself makes them also important as transport forms of cholesterol. In addition, oxysterols have a number of important functions in connection with cholesterol turnover, atherosclerosis, apoptosis, necrosis, inflammation, immunosuppression, and the development of gallstones. They are present in cells at very low concentrations when compared to cholesterol. It has been suggested that side-chain oxidized oxysterols mediate a number of effects when cellular cholesterol levels increase. When added to cells *in vitro*, oxysterols alter cholesterol homeostasis. They accomplish this goal by binding to the ER anchor protein insulin induced gene1 (INSIG1), which then binds to and retains sterol regulatory element-binding protein cleavage-activating protein (SCAP)/ sterol regulatory element-binding protein (SREBP) complexes in the ER. Consequently, the transport of SREBP at the Golgi is impaired, resulting in reduced nuclear levels of the transcriptional active SREBP fragment. Oxysterol/ INSIG1 complex also increases the degradation of HMG CoA reductase, the rate-limiting enzyme of cholesterol biosynthesis. In addition, many oxysterols are endogenous LXR agonists.

Numbers of *in vitro* studies show that elevated oxysterol levels are cytotoxic and atherogenic. Clinical studies show that increased levels of LDL

cholesterol promote premature atherosclerosis. According to the oxidative modification hypothesis, LDL in its native state is not atherogenic. Oxidatively modified LDL contains elevated levels of 7-ketocholesterol, 7-hydroxycholesterol and other 5,6-oxygenated sterols. The primary 7-oxygenated products of cholesterol, 7-ketocholesterol and 7-hydroperoxycholesterol, seem to be the most cytotoxic oxygenated lipid present in oxidized LDL. Excessive uptake of oxLDL is a decisive process in the formation of atherosclerosis lesion.

As we discussed earlier that ABCG1 plays an important role in macrophage lipid metabolism and atherosclerosis. Baldan *et al* observed a significant decrease in lesion size in *Ldlr*^{-/-} mice receiving *Abcg1*^{-/-} bone marrow cells. The authors proposed that the smaller lesion was a result of increased apoptosis of the *Abcg1*^{-/-} macrophages that are abundant in the atherosclerosis lesion of *Ldlr*^{-/-} mice (Baldan et al., 2006). The role for ABCG1 in protection against apoptosis is consistent with the study by Terasaka *et al* that overexpression of ABCG1 in cultured cells attenuates oxysterol-induced cell death because of the stimulated efflux of 7-ketocholesterol to exogenous HDL. They reported that the protection against oxLDL-induced apoptosis in macrophages is specifically dependent on ABCG1/HDL since ABCG1 is able to promote efflux of 7-ketocholesterol from cells onto HDL.

Our data support the *in vivo* studies that ABCG1 can function as a transporter of oxysterols, such as 7-ketocholesterol. Based on our findings, the detailed mechanisms by which ABCG1 regulates the efflux of cholesterol and 7-ketocholesterol might be different. Thus, we will need to not only study the

detailed mechanisms of how ABCG1 works as a transporter for cholesterol but also investigate how it regulates oxysterol translocation and whether there are other potential substrates for ABCG1.

Reference

- Abildayeva, K., Jansen, P.J., Hirsch-Reinshagen, V., Bloks, V.W., Bakker, A.H., Ramaekers, F.C., de Vente, J., Groen, A.K., Wellington, C.L., Kuipers, F., and Mulder, M. (2006). 24(S)-hydroxycholesterol participates in a liver X receptor-controlled pathway in astrocytes that regulates apolipoprotein E-mediated cholesterol efflux. *The Journal of biological chemistry* 281, 12799-12808.
- Amaral, J., Lee, J.W., Chou, J., Campos, M.M., and Rodriguez, I.R. (2013). 7-Ketocholesterol induces inflammation and angiogenesis in vivo: a novel rat model. *PloS one* 8, e56099.
- Asztalos, B.F., Collins, D., Cupples, L.A., Demissie, S., Horvath, K.V., Bloomfield, H.E., Robins, S.J., and Schaefer, E.J. (2005). Value of high-density lipoprotein (HDL) subpopulations in predicting recurrent cardiovascular events in the Veterans Affairs HDL Intervention Trial. *Arteriosclerosis, thrombosis, and vascular biology* 25, 2185-2191.
- Baekkeskov, S., and Kanaani, J. (2009). Palmitoylation cycles and regulation of protein function (Review). *Mol Membr Biol* 26, 42-54.
- Baldan, A., Gomes, A.V., Ping, P., and Edwards, P.A. (2008). Loss of ABCG1 results in chronic pulmonary inflammation. *J Immunol* 180, 3560-3568.
- Baldan, A., Pei, L., Lee, R., Tarr, P., Tangirala, R.K., Weinstein, M.M., Frank, J., Li, A.C., Tontonoz, P., and Edwards, P.A. (2006). Impaired development of atherosclerosis in hyperlipidemic *Ldlr*^{-/-} and *ApoE*^{-/-} mice transplanted

with Abcg1^{-/-} bone marrow. Arteriosclerosis, thrombosis, and vascular biology 26, 2301-2307.

Barter, P., Gotto, A.M., LaRosa, J.C., Maroni, J., Szarek, M., Grundy, S.M., Kastelein, J.J., Bittner, V., and Fruchart, J.C. (2007). HDL cholesterol, very low levels of LDL cholesterol, and cardiovascular events. The New England journal of medicine 357, 1301-1310.

Bell, J.A., Becktel, W.J., Sauer, U., Baase, W.A., and Matthews, B.W. (1992). Dissection of helix capping in T4 lysozyme by structural and thermodynamic analysis of six amino acid substitutions at Thr 59. Biochemistry 31, 3590-3596.

Berge, K.E., Tian, H., Graf, G.A., Yu, L., Grishin, N.V., Schultz, J., Kwiterovich, P., Shan, B., Barnes, R., and Hobbs, H.H. (2000). Accumulation of dietary cholesterol in sitosterolemia caused by mutations in adjacent ABC transporters. Science 290, 1771-1775.

Beyea, M.M., Heslop, C.L., Sawyez, C.G., Edwards, J.Y., Markle, J.G., Hegele, R.A., and Huff, M.W. (2007). Selective up-regulation of LXR-regulated genes ABCA1, ABCG1, and APOE in macrophages through increased endogenous synthesis of 24(S),25-epoxycholesterol. The Journal of biological chemistry 282, 5207-5216.

Biemans-Oldehinkel, E., Doeven, M.K., and Poolman, B. (2006). ABC transporter architecture and regulatory roles of accessory domains. FEBS letters 580, 1023-1035.

Brooks-Wilson, A., Marcil, M., Clee, S.M., Zhang, L.H., Roomp, K., van Dam, M., Yu, L., Brewer, C., Collins, J.A., Molhuizen, H.O., Loubser, O., Ouelette, B.F., Fichter, K., Ashbourne-Excoffon, K.J., Sensen, C.W., Scherer, S., Mott, S., Denis, M., Martindale, D., Frohlich, J., Morgan, K., Koop, B., Pimstone, S., Kastelein, J.J., Genest, J., Jr., and Hayden, M.R. (1999). Mutations in ABC1 in Tangier disease and familial high-density lipoprotein deficiency. *Nature genetics* 22, 336-345.

Buettner, R., Mora, L.B., and Jove, R. (2002). Activated STAT signaling in human tumors provides novel molecular targets for therapeutic intervention. *Clinical cancer research : an official journal of the American Association for Cancer Research* 8, 945-954.

Burgess, B., Naus, K., Chan, J., Hirsch-Reinshagen, V., Tansley, G., Matzke, L., Chan, B., Wilkinson, A., Fan, J., Donkin, J., Balik, D., Tanaka, T., Ou, G., Dyer, R., Innis, S., McManus, B., Lutjohann, D., and Wellington, C. (2008). Overexpression of human ABCG1 does not affect atherosclerosis in fat-fed ApoE-deficient mice. *Arteriosclerosis, thrombosis, and vascular biology* 28, 1731-1737.

Chang, X.B. (2007). A molecular understanding of ATP-dependent solute transport by multidrug resistance-associated protein MRP1. *Cancer metastasis reviews* 26, 15-37.

Charollais, J., and Van Der Goot, F.G. (2009). Palmitoylation of membrane proteins (Review). *Mol Membr Biol* 26, 55-66.

Chen, J., Lu, G., Lin, J., Davidson, A.L., and Quioco, F.A. (2003). A tweezers-like motion of the ATP-binding cassette dimer in an ABC transport cycle. *Molecular cell* 12, 651-661.

Cheng, S.H., Gregory, R.J., Marshall, J., Paul, S., Souza, D.W., White, G.A., O'Riordan, C.R., and Smith, A.E. (1990). Defective intracellular transport and processing of CFTR is the molecular basis of most cystic fibrosis. *Cell* 63, 827-834.

Chroni, A., Liu, T., Fitzgerald, M.L., Freeman, M.W., and Zannis, V.I. (2004). Cross-linking and lipid efflux properties of apoA-I mutants suggest direct association between apoA-I helices and ABCA1. *Biochemistry* 43, 2126-2139.

Cserepes, J., Szentpetery, Z., Seres, L., Ozvegy-Laczka, C., Langmann, T., Schmitz, G., Glavinas, H., Klein, I., Homolya, L., Varadi, A., Sarkadi, B., and Elkind, N.B. (2004). Functional expression and characterization of the human ABCG1 and ABCG4 proteins: indications for heterodimerization. *Biochem Biophys Res Commun* 320, 860-867.

Daoud, R., Julien, M., Gros, P., and Georges, E. (2001). Major photoaffinity drug binding sites in multidrug resistance protein 1 (MRP1) are within transmembrane domains 10-11 and 16-17. *The Journal of biological chemistry* 276, 12324-12330.

Dean, M.C. (2002). The human ATP-binding cassette (ABC) transporter superfamily. ([Bethesda, MD: NCBI]).

Deeley, R.G., Westlake, C., and Cole, S.P. (2006). Transmembrane transport of endo- and xenobiotics by mammalian ATP-binding cassette multidrug resistance proteins. *Physiological reviews* 86, 849-899.

Diederichs, K., Diez, J., Greller, G., Muller, C., Breed, J., Schnell, C., Vonnrhein, C., Boos, W., and Welte, W. (2000). Crystal structure of MalK, the ATPase subunit of the trehalose/maltose ABC transporter of the archaeon *Thermococcus litoralis*. *The EMBO journal* 19, 5951-5961.

Engel, T., Bode, G., Lueken, A., Knop, M., Kannenberg, F., Nofer, J.R., Assmann, G., and Seedorf, U. (2006). Expression and functional characterization of ABCG1 splice variant ABCG1(666). *FEBS letters* 580, 4551-4559.

Farhan, H., Reiterer, V., Korkhov, V.M., Schmid, J.A., Freissmuth, M., and Sitte, H.H. (2007). Concentrative export from the endoplasmic reticulum of the gamma-aminobutyric acid transporter 1 requires binding to SEC24D. *J Biol Chem* 282, 7679-7689.

Fitzgerald, M.L., Morris, A.L., Chroni, A., Mendez, A.J., Zannis, V.I., and Freeman, M.W. (2004). ABCA1 and amphipathic apolipoproteins form high-affinity molecular complexes required for cholesterol efflux. *J Lipid Res* 45, 287-294.

Fitzgerald, M.L., Morris, A.L., Rhee, J.S., Andersson, L.P., Mendez, A.J., and Freeman, M.W. (2002). Naturally occurring mutations in the largest extracellular loops of ABCA1 can disrupt its direct interaction with apolipoprotein A-I. *J Biol Chem* 277, 33178-33187.

Fryirs, M.A., Barter, P.J., Appavoo, M., Tuch, B.E., Tabet, F., Heather, A.K., and Rye, K.A. (2010). Effects of high-density lipoproteins on pancreatic beta-cell insulin secretion. *Arteriosclerosis, thrombosis, and vascular biology* 30, 1642-1648.

Gao, M., Loe, D.W., Grant, C.E., Cole, S.P., and Deeley, R.G. (1996). Reconstitution of ATP-dependent leukotriene C4 transport by Co-expression of both half-molecules of human multidrug resistance protein in insect cells. *The Journal of biological chemistry* 271, 27782-27787.

Gao, X., Gu, H., Li, G., Rye, K.A., and Zhang, D.W. (2012). Identification of an amino acid residue in ATP-binding cassette transport G1 critical for mediating cholesterol efflux. *Biochimica et biophysica acta* 1821, 552-559.

Gaudet, R., and Wiley, D.C. (2001). Structure of the ABC ATPase domain of human TAP1, the transporter associated with antigen processing. *The EMBO journal* 20, 4964-4972.

Gelissen, I.C., Harris, M., Rye, K.A., Quinn, C., Brown, A.J., Kockx, M., Cartland, S., Packianathan, M., Kritharides, L., and Jessup, W. (2006). ABCA1 and ABCG1 synergize to mediate cholesterol export to apoA-I. *Arteriosclerosis, thrombosis, and vascular biology* 26, 534-540.

Graf, G.A., Yu, L., Li, W.P., Gerard, R., Tuma, P.L., Cohen, J.C., and Hobbs, H.H. (2003). ABCG5 and ABCG8 are obligate heterodimers for protein trafficking and biliary cholesterol excretion. *The Journal of biological chemistry* 278, 48275-48282.

Greaves, J., Prescott, G.R., Gorleku, O.A., and Chamberlain, L.H. (2009). The fat controller: roles of palmitoylation in intracellular protein trafficking and targeting to membrane microdomains (Review). *Mol Membr Biol* 26, 67-79.

Gu, H.M., Li, G., Gao, X., Berthiaume, L.G., and Zhang, D.W. (2013). Characterization of palmitoylation of ATP binding cassette transporter G1: Effect on protein trafficking and function. *Biochimica et biophysica acta* 1831, 1067-1078.

Higgins, C.F. (2007). Multiple molecular mechanisms for multidrug resistance transporters. *Nature* 446, 749-757.

Higgins, C.F., and Linton, K.J. (2004). The ATP switch model for ABC transporters. *Nature structural & molecular biology* 11, 918-926.

Hirayama, H., Kimura, Y., Kioka, N., Matsuo, M., and Ueda, K. (2012). ATPase activity of human ABCG1 is stimulated by cholesterol and sphingomyelin. *Journal of lipid research*.

Hollingworth, P., Harold, D., Sims, R., Gerrish, A., Lambert, J.C., Carrasquillo, M.M., Abraham, R., Hamshere, M.L., Pahwa, J.S., Moskvina, V., Dowzell, K., Jones, N., Stretton, A., Thomas, C., Richards, A., Ivanov, D., Widdowson, C., Chapman, J., Lovestone, S., Powell, J., Proitsi, P., Lupton, M.K., Brayne, C., Rubinsztein, D.C., Gill, M., Lawlor, B., Lynch, A., Brown, K.S., Passmore, P.A., Craig, D., McGuinness, B., Todd, S., Holmes, C., Mann, D., Smith, A.D., Beaumont, H., Warden, D., Wilcock, G., Love, S., Kehoe, P.G., Hooper, N.M., Vardy, E.R., Hardy, J., Mead, S., Fox, N.C., Rossor, M., Collinge, J., Maier, W., Jessen, F., Ruther, E., Schurmann, B., Heun, R., Kolsch, H., van den Bussche, H.,

Heuser, I., Kornhuber, J., Wiltfang, J., Dichgans, M., Frolich, L., Hampel, H., Gallacher, J., Hull, M., Rujescu, D., Giegling, I., Goate, A.M., Kauwe, J.S., Cruchaga, C., Nowotny, P., Morris, J.C., Mayo, K., Sleegers, K., Bettens, K., Engelborghs, S., De Deyn, P.P., Van Broeckhoven, C., Livingston, G., Bass, N.J., Gurling, H., McQuillin, A., Gwilliam, R., Deloukas, P., Al-Chalabi, A., Shaw, C.E., Tzolaki, M., Singleton, A.B., Guerreiro, R., Muhleisen, T.W., Nothen, M.M., Moebus, S., Jockel, K.H., Klopp, N., Wichmann, H.E., Pankratz, V.S., Sando, S.B., Aasly, J.O., Barcikowska, M., Wszolek, Z.K., Dickson, D.W., Graff-Radford, N.R., Petersen, R.C., van Duijn, C.M., Breteler, M.M., Ikram, M.A., DeStefano, A.L., Fitzpatrick, A.L., Lopez, O., Launer, L.J., Seshadri, S., Berr, C., Champion, D., Epelbaum, J., Dartigues, J.F., Tzourio, C., Alperovitch, A., Lathrop, M., Feulner, T.M., Friedrich, P., Riehle, C., Krawczak, M., Schreiber, S., Mayhaus, M., Nicolhaus, S., Wagenpfeil, S., Steinberg, S., Stefansson, H., Stefansson, K., Snaedal, J., Bjornsson, S., Jonsson, P.V., Chouraki, V., Genier-Boley, B., Hiltunen, M., Soininen, H., Combarros, O., Zelenika, D., Delepine, M., Bullido, M.J., Pasquier, F., Mateo, I., Frank-Garcia, A., Porcellini, E., Hanon, O., Coto, E., Alvarez, V., Bosco, P., Siciliano, G., Mancuso, M., Panza, F., Solfrizzi, V., Nacmias, B., Sorbi, S., Bossu, P., Piccardi, P., Arosio, B., Annoni, G., Seripa, D., Pilotto, A., Scarpini, E., Galimberti, D., Brice, A., Hannequin, D., Licastro, F., Jones, L., Holmans, P.A., Jonsson, T., Riemenschneider, M., Morgan, K., Younkin, S.G., Owen, M.J., O'Donovan, M., Amouyel, P., and Williams, J. (2011). Common variants at ABCA7, MS4A6A/MS4A4E, EPHA1, CD33 and CD2AP are associated with Alzheimer's disease. *Nature genetics* 43, 429-435.

Hung, L.W., Wang, I.X., Nikaido, K., Liu, P.Q., Ames, G.F., and Kim, S.H. (1998). Crystal structure of the ATP-binding subunit of an ABC transporter. *Nature* 396, 703-707.

Jakobsson, T., Venteclef, N., Toresson, G., Damdimopoulos, A.E., Ehrlund, A., Lou, X., Sanyal, S., Steffensen, K.R., Gustafsson, J.A., and Treuter, E. (2009). GPS2 is required for cholesterol efflux by triggering histone demethylation, LXR recruitment, and coregulator assembly at the ABCG1 locus. *Molecular cell* 34, 510-518.

Karpowich, N., Martsinkevich, O., Millen, L., Yuan, Y.R., Dai, P.L., MacVey, K., Thomas, P.J., and Hunt, J.F. (2001). Crystal structures of the MJ1267 ATP binding cassette reveal an induced-fit effect at the ATPase active site of an ABC transporter. *Structure (London, England : 1993)* 9, 571-586.

Karwatsky, J., Leimanis, M., Cai, J., Gros, P., and Georges, E. (2005). The leucotriene C4 binding sites in multidrug resistance protein 1 (ABCC1) include the first membrane multiple spanning domain. *Biochemistry* 44, 340-351.

Kennedy, M.A., Barrera, G.C., Nakamura, K., Baldan, A., Tarr, P., Fishbein, M.C., Frank, J., Francone, O.L., and Edwards, P.A. (2005). ABCG1 has a critical role in mediating cholesterol efflux to HDL and preventing cellular lipid accumulation. *Cell Metab* 1, 121-131.

Kennedy, M.A., Venkateswaran, A., Tarr, P.T., Xenarios, I., Kudoh, J., Shimizu, N., and Edwards, P.A. (2001). Characterization of the human ABCG1 gene: liver X receptor activates an internal promoter that produces a novel

transcript encoding an alternative form of the protein. *The Journal of biological chemistry* 276, 39438-39447.

Klucken, J., Buchler, C., Orso, E., Kaminski, W.E., Porsch-Ozcurumez, M., Liebisch, G., Kapinsky, M., Diederich, W., Drobnik, W., Dean, M., Allikmets, R., and Schmitz, G. (2000). ABCG1 (ABC8), the human homolog of the *Drosophila* white gene, is a regulator of macrophage cholesterol and phospholipid transport. *Proceedings of the National Academy of Sciences of the United States of America* 97, 817-822.

Kobayashi, A., Takanezawa, Y., Hirata, T., Shimizu, Y., Misasa, K., Kioka, N., Arai, H., Ueda, K., and Matsuo, M. (2006). Efflux of sphingomyelin, cholesterol, and phosphatidylcholine by ABCG1. *Journal of lipid research* 47, 1791-1802.

Koike, K., Conseil, G., Leslie, E.M., Deeley, R.G., and Cole, S.P. (2004). Identification of proline residues in the core cytoplasmic and transmembrane regions of multidrug resistance protein 1 (MRP1/ABCC1) important for transport function, substrate specificity, and nucleotide interactions. *The Journal of biological chemistry* 279, 12325-12336.

Kruit, J.K., Wijesekara, N., Westwell-Roper, C., Vanmierlo, T., de Haan, W., Bhattacharjee, A., Tang, R., Wellington, C.L., Lutjohann, D., Johnson, J.D., Brunham, L.R., Verchere, C.B., and Hayden, M.R. (2012). Loss of both ABCA1 and ABCG1 results in increased disturbances in islet sterol homeostasis, inflammation, and impaired beta-cell function. *Diabetes* 61, 659-664.

Larrede, S., Quinn, C.M., Jessup, W., Frisdal, E., Olivier, M., Hsieh, V., Kim, M.J., Van Eck, M., Couvert, P., Carrie, A., Giral, P., Chapman, M.J., Guerin, M., and Le

Goff, W. (2009). Stimulation of Cholesterol Efflux by LXR Agonists in Cholesterol-Loaded Human Macrophages Is ABCA1-Dependent but ABCG1-Independent. *Arteriosclerosis, thrombosis, and vascular biology*.

Leimanis, M.L., and Georges, E. (2007). ABCG2 membrane transporter in mature human erythrocytes is exclusively homodimer. *Biochem Biophys Res Commun* 354, 345-350.

Letourneau, I.J., Nakajima, A., Deeley, R.G., and Cole, S.P. (2008). Role of proline 1150 in functional interactions between the membrane spanning domains and nucleotide binding domains of the MRP1 (ABCC1) transporter. *Biochemical pharmacology* 75, 1659-1669.

Levy, D.E., and Darnell, J.E., Jr. (2002). Stats: transcriptional control and biological impact. *Nature reviews. Molecular cell biology* 3, 651-662.

Li, A.C., Binder, C.J., Gutierrez, A., Brown, K.K., Plotkin, C.R., Pattison, J.W., Valledor, A.F., Davis, R.A., Willson, T.M., Witztum, J.L., Palinski, W., and Glass, C.K. (2004). Differential inhibition of macrophage foam-cell formation and atherosclerosis in mice by PPARalpha, beta/delta, and gamma. *J Clin Invest* 114, 1564-1576.

Liu, Y., and Tang, C. (2012). Regulation of ABCA1 functions by signaling pathways. *Biochimica et biophysica acta* 1821, 522-529.

Loo, T.W., and Clarke, D.M. (1997). Correction of defective protein kinesis of human P-glycoprotein mutants by substrates and modulators. *J Biol Chem* 272, 709-712.

Loo, T.W., and Clarke, D.M. (2005). Recent progress in understanding the mechanism of P-glycoprotein-mediated drug efflux. *J Membr Biol* 206, 173-185.

Loo, T.W., and Clarke, D.M. (2008). Mutational analysis of ABC proteins. *Arch Biochem Biophys* 476, 51-64.

Lorkowski, S., Kratz, M., Wenner, C., Schmidt, R., Weitkamp, B., Fobker, M., Reinhardt, J., Rauterberg, J., Galinski, E.A., and Cullen, P. (2001). Expression of the ATP-binding cassette transporter gene ABCG1 (ABC8) in Tangier disease. *Biochem Biophys Res Commun* 283, 821-830.

Mancias, J.D., and Goldberg, J. (2008). Structural basis of cargo membrane protein discrimination by the human COPII coat machinery. *EMBO J* 27, 2918-2928.

Mauldin, J.P., Nagelin, M.H., Wojcik, A.J., Srinivasan, S., Skafien, M.D., Ayers, C.R., McNamara, C.A., and Hedrick, C.C. (2008). Reduced expression of ATP-binding cassette transporter G1 increases cholesterol accumulation in macrophages of patients with type 2 diabetes mellitus. *Circulation* 117, 2785-2792.

Mauldin, J.P., Srinivasan, S., Mulya, A., Gebre, A., Parks, J.S., Daugherty, A., and Hedrick, C.C. (2006). Reduction in ABCG1 in Type 2 diabetic mice increases macrophage foam cell formation. *The Journal of biological chemistry* 281, 21216-21224.

McNeish, J., Aiello, R.J., Guyot, D., Turi, T., Gabel, C., Aldinger, C., Hoppe, K.L., Roach, M.L., Royer, L.J., de Wet, J., Broccardo, C., Chimini, G., and Francone,

O.L. (2000). High density lipoprotein deficiency and foam cell accumulation in mice with targeted disruption of ATP-binding cassette transporter-1. *Proceedings of the National Academy of Sciences of the United States of America* 97, 4245-4250.

Meurs, I., Lammers, B., Zhao, Y., Out, R., Hildebrand, R.B., Hoekstra, M., Van Berkel, T.J., and Van Eck, M. (2012). The effect of ABCG1 deficiency on atherosclerotic lesion development in LDL receptor knockout mice depends on the stage of atherogenesis. *Atherosclerosis* 221, 41-47.

Moitra, K., and Dean, M. (2011). Evolution of ABC transporters by gene duplication and their role in human disease. *Biological chemistry* 392, 29-37.

Nieland, T.J., Chroni, A., Fitzgerald, M.L., Maliga, Z., Zannis, V.I., Kirchhausen, T., and Krieger, M. (2004). Cross-inhibition of SR-BI- and ABCA1-mediated cholesterol transport by the small molecules BLT-4 and glyburide. *Journal of lipid research* 45, 1256-1265.

Oram, J.F., and Vaughan, A.M. (2006). ATP-Binding cassette cholesterol transporters and cardiovascular disease. *Circulation research* 99, 1031-1043.

Orso, E., Broccardo, C., Kaminski, W.E., Bottcher, A., Liebisch, G., Drobnik, W., Gotz, A., Chambenoit, O., Diederich, W., Langmann, T., Spruss, T., Luciani, M.F., Rothe, G., Lackner, K.J., Chimini, G., and Schmitz, G. (2000). Transport of lipids from golgi to plasma membrane is defective in tangier disease patients and Abc1-deficient mice. *Nature genetics* 24, 192-196.

Oswald, C., Holland, I.B., and Schmitt, L. (2006). The motor domains of ABC-transporters. What can structures tell us? *Naunyn-Schmiedeberg's archives of pharmacology* 372, 385-399.

Out, R., Hoekstra, M., Habets, K., Meurs, I., de Waard, V., Hildebrand, R.B., Wang, Y., Chimini, G., Kuiper, J., Van Berkel, T.J., and Van Eck, M. (2008a). Combined deletion of macrophage ABCA1 and ABCG1 leads to massive lipid accumulation in tissue macrophages and distinct atherosclerosis at relatively low plasma cholesterol levels. *Arteriosclerosis, thrombosis, and vascular biology* 28, 258-264.

Out, R., Hoekstra, M., Hildebrand, R.B., Kruit, J.K., Meurs, I., Li, Z., Kuipers, F., Van Berkel, T.J., and Van Eck, M. (2006). Macrophage ABCG1 deletion disrupts lipid homeostasis in alveolar macrophages and moderately influences atherosclerotic lesion development in LDL receptor-deficient mice. *Arteriosclerosis, thrombosis, and vascular biology* 26, 2295-2300.

Out, R., Hoekstra, M., Meurs, I., de Vos, P., Kuiper, J., Van Eck, M., and Van Berkel, T.J. (2007). Total body ABCG1 expression protects against early atherosclerotic lesion development in mice. *Arteriosclerosis, thrombosis, and vascular biology* 27, 594-599.

Out, R., Jessup, W., Le Goff, W., Hoekstra, M., Gelissen, I.C., Zhao, Y., Kritharides, L., Chimini, G., Kuiper, J., Chapman, M.J., Huby, T., Van Berkel, T.J., and Van Eck, M. (2008b). Coexistence of foam cells and hypocholesterolemia in mice lacking the ABC transporters A1 and G1. *Circulation research* 102, 113-120.

Patel, S., Drew, B.G., Nakhla, S., Duffy, S.J., Murphy, A.J., Barter, P.J., Rye, K.A., Chin-Dusting, J., Hoang, A., Sviridov, D., Celermajer, D.S., and Kingwell, B.A. (2009). Reconstituted high-density lipoprotein increases plasma high-density lipoprotein anti-inflammatory properties and cholesterol efflux capacity in patients with type 2 diabetes. *Journal of the American College of Cardiology* 53, 962-971.

Ranalletta, M., Wang, N., Han, S., Yvan-Charvet, L., Welch, C., and Tall, A.R. (2006). Decreased atherosclerosis in low-density lipoprotein receptor knockout mice transplanted with *Abcg1*^{-/-} bone marrow. *Arteriosclerosis, thrombosis, and vascular biology* 26, 2308-2315.

Rees, D.C., Johnson, E., and Lewinson, O. (2009). ABC transporters: the power to change. *Nature reviews. Molecular cell biology* 10, 218-227.

Richardson, J.S., and Richardson, D.C. (1988). Amino acid preferences for specific locations at the ends of alpha helices. *Science* 240, 1648-1652.

Rohrer, L., Ohnsorg, P.M., Lehner, M., Landolt, F., Rinninger, F., and von Eckardstein, A. (2009). High-density lipoprotein transport through aortic endothelial cells involves scavenger receptor BI and ATP-binding cassette transporter G1. *Circulation research* 104, 1142-1150.

Rosenson, R.S., Brewer, H.B., Jr., Davidson, W.S., Fayad, Z.A., Fuster, V., Goldstein, J., Hellerstein, M., Jiang, X.C., Phillips, M.C., Rader, D.J., Remaley, A.T., Rothblat, G.H., Tall, A.R., and Yvan-Charvet, L. (2012). Cholesterol efflux and atheroprotection: advancing the concept of reverse cholesterol transport. *Circulation* 125, 1905-1919.

Sano, O., Kobayashi, A., Nagao, K., Kumagai, K., Kioka, N., Hanada, K., Ueda, K., and Matsuo, M. (2007). Sphingomyelin-dependence of cholesterol efflux mediated by ABCG1. *Journal of lipid research* 48, 2377-2384.

Seeger, M.A., and van Veen, H.W. (2009). Molecular basis of multidrug transport by ABC transporters. *Biochimica et biophysica acta* 1794, 725-737.

Seres, L., Cserepes, J., Elkind, N.B., Torocsik, D., Nagy, L., Sarkadi, B., and Homolya, L. (2008). Functional ABCG1 expression induces apoptosis in macrophages and other cell types. *Biochimica et biophysica acta* 1778, 2378-2387.

Serrano, L., Bycroft, M., and Fersht, A.R. (1991). Aromatic-aromatic interactions and protein stability. Investigation by double-mutant cycles. *J Mol Biol* 218, 465-475.

Serrano, L., Sancho, J., Hirshberg, M., and Fersht, A.R. (1992). Alpha-helix stability in proteins. I. Empirical correlations concerning substitution of side-chains at the N and C-caps and the replacement of alanine by glycine or serine at solvent-exposed surfaces. *J Mol Biol* 227, 544-559.

Sharom, F.J. (2008). ABC multidrug transporters: structure, function and role in chemoresistance. *Pharmacogenomics* 9, 105-127.

Silva, C.M. (2004). Role of STATs as downstream signal transducers in Src family kinase-mediated tumorigenesis. *Oncogene* 23, 8017-8023.

Singaraja, R.R., Fievet, C., Castro, G., James, E.R., Hennuyer, N., Clee, S.M., Bissada, N., Choy, J.C., Fruchart, J.C., McManus, B.M., Staels, B., and Hayden,

M.R. (2002). Increased ABCA1 activity protects against atherosclerosis. *J Clin Invest* 110, 35-42.

Singaraja, R.R., Van Eck, M., Bissada, N., Zimetti, F., Collins, H.L., Hildebrand, R.B., Hayden, A., Brunham, L.R., Kang, M.H., Fruchart, J.C., Van Berkel, T.J., Parks, J.S., Staels, B., Rothblat, G.H., Fievet, C., and Hayden, M.R. (2006). Both hepatic and extrahepatic ABCA1 have discrete and essential functions in the maintenance of plasma high-density lipoprotein cholesterol levels in vivo. *Circulation* 114, 1301-1309.

Smith, J.D., Le Goff, W., Settle, M., Brubaker, G., Waelde, C., Horwitz, A., and Oda, M.N. (2004). ABCA1 mediates concurrent cholesterol and phospholipid efflux to apolipoprotein A-I. *Journal of lipid research* 45, 635-644.

Smith, P.C., Karpowich, N., Millen, L., Moody, J.E., Rosen, J., Thomas, P.J., and Hunt, J.F. (2002). ATP binding to the motor domain from an ABC transporter drives formation of a nucleotide sandwich dimer. *Molecular cell* 10, 139-149.

Sturek, J.M., Castle, J.D., Trace, A.P., Page, L.C., Castle, A.M., Evans-Molina, C., Parks, J.S., Mirmira, R.G., and Hedrick, C.C. (2010). An intracellular role for ABCG1-mediated cholesterol transport in the regulated secretory pathway of mouse pancreatic beta cells. *J Clin Invest* 120, 2575-2589.

Sucic, S., El-Kasaby, A., Kudlacek, O., Sarker, S., Sitte, H.H., Marin, P., and Freissmuth, M. (2011). The serotonin transporter is an exclusive client of the coat protein complex II (COPII) component SEC24C. *J Biol Chem* 286, 16482-16490.

Tang, C., Liu, Y., Kessler, P.S., Vaughan, A.M., and Oram, J.F. (2009). The macrophage cholesterol exporter ABCA1 functions as an anti-inflammatory receptor. *The Journal of biological chemistry* 284, 32336-32343.

Tarling, E.J., and Edwards, P.A. (2011). ATP binding cassette transporter G1 (ABCG1) is an intracellular sterol transporter. *Proceedings of the National Academy of Sciences of the United States of America* 108, 19719-19724.

Terasaka, N., Wang, N., Yvan-Charvet, L., and Tall, A.R. (2007). High-density lipoprotein protects macrophages from oxidized low-density lipoprotein-induced apoptosis by promoting efflux of 7-ketocholesterol via ABCG1. *Proceedings of the National Academy of Sciences of the United States of America* 104, 15093-15098.

Terasaka, N., Westerterp, M., Koetsveld, J., Fernandez-Hernando, C., Yvan-Charvet, L., Wang, N., Sessa, W.C., and Tall, A.R. (2010). ATP-binding cassette transporter G1 and high-density lipoprotein promote endothelial NO synthesis through a decrease in the interaction of caveolin-1 and endothelial NO synthase. *Arteriosclerosis, thrombosis, and vascular biology* 30, 2219-2225.

Vaughan, A.M., and Oram, J.F. (2005). ABCG1 redistributes cell cholesterol to domains removable by high density lipoprotein but not by lipid-depleted apolipoproteins. *The Journal of biological chemistry* 280, 30150-30157.

Vaughan, A.M., and Oram, J.F. (2006). ABCA1 and ABCG1 or ABCG4 act sequentially to remove cellular cholesterol and generate cholesterol-rich HDL. *Journal of lipid research* 47, 2433-2443.

Wang, N., Lan, D., Chen, W., Matsuura, F., and Tall, A.R. (2004). ATP-binding cassette transporters G1 and G4 mediate cellular cholesterol efflux to high-density lipoproteins. *Proceedings of the National Academy of Sciences of the United States of America* 101, 9774-9779.

Wang, N., Ranalletta, M., Matsuura, F., Peng, F., and Tall, A.R. (2006a). LXR-induced redistribution of ABCG1 to plasma membrane in macrophages enhances cholesterol mass efflux to HDL. *Arteriosclerosis, thrombosis, and vascular biology* 26, 1310-1316.

Wang, N., Silver, D.L., Costet, P., and Tall, A.R. (2000). Specific binding of ApoA-I, enhanced cholesterol efflux, and altered plasma membrane morphology in cells expressing ABC1. *J Biol Chem* 275, 33053-33058.

Wang, X., Collins, H.L., Ranalletta, M., Fuki, I.V., Billheimer, J.T., Rothblat, G.H., Tall, A.R., and Rader, D.J. (2007). Macrophage ABCA1 and ABCG1, but not SR-BI, promote macrophage reverse cholesterol transport in vivo. *J Clin Invest* 117, 2216-2224.

Wang, Z., Stalcup, L.D., Harvey, B.J., Weber, J., Chloupkova, M., Dumont, M.E., Dean, M., and Urbatsch, I.L. (2006b). Purification and ATP hydrolysis of the putative cholesterol transporters ABCG5 and ABCG8. *Biochemistry* 45, 9929-9939.

Wendeler, M.W., Paccaud, J.P., and Hauri, H.P. (2007). Role of Sec24 isoforms in selective export of membrane proteins from the endoplasmic reticulum. *EMBO Rep* 8, 258-264.

Westerterp, M., Koetsveld, J., Yu, S., Han, S., Li, R., Goldberg, I.J., Welch, C.L., and Tall, A.R. (2010). Increased Atherosclerosis in Mice With Vascular ATP-Binding Cassette Transporter G1 Deficiency--Brief Report. *Arteriosclerosis, thrombosis, and vascular biology*.

Wiersma, H., Nijstad, N., de Boer, J.F., Out, R., Hogewerf, W., Van Berkel, T.J., Kuipers, F., and Tietge, U.J. (2009). Lack of Abcg1 results in decreased plasma HDL cholesterol levels and increased biliary cholesterol secretion in mice fed a high cholesterol diet. *Atherosclerosis* 206, 141-147.

Williams, L.M., Sarma, U., Willets, K., Smallie, T., Brennan, F., and Foxwell, B.M. (2007). Expression of constitutively active STAT3 can replicate the cytokine-suppressive activity of interleukin-10 in human primary macrophages. *The Journal of biological chemistry* 282, 6965-6975.

Wojcik, A.J., Skaflen, M.D., Srinivasan, S., and Hedrick, C.C. (2008). A critical role for ABCG1 in macrophage inflammation and lung homeostasis. *J Immunol* 180, 4273-4282.

Xie, Q., Engel, T., Schnoor, M., Niehaus, J., Hofnagel, O., Buers, I., Cullen, P., Seedorf, U., Assmann, G., and Lorkowski, S. (2006). Cell surface localization of ABCG1 does not require LXR activation. *Arteriosclerosis, thrombosis, and vascular biology* 26, e143-144; author reply e145.

Xu, J., Liu, Y., Yang, Y., Bates, S., and Zhang, J.T. (2004). Characterization of oligomeric human half-ABC transporter ATP-binding cassette G2. *The Journal of biological chemistry* 279, 19781-19789.

Yu, H., and Jove, R. (2004). The STATs of cancer--new molecular targets come of age. *Nature reviews. Cancer* 4, 97-105.

Yu, L., Hammer, R.E., Li-Hawkins, J., Von Bergmann, K., Lutjohann, D., Cohen, J.C., and Hobbs, H.H. (2002a). Disruption of *Abcg5* and *Abcg8* in mice reveals their crucial role in biliary cholesterol secretion. *Proceedings of the National Academy of Sciences of the United States of America* 99, 16237-16242.

Yu, L., Li-Hawkins, J., Hammer, R.E., Berge, K.E., Horton, J.D., Cohen, J.C., and Hobbs, H.H. (2002b). Overexpression of *ABCG5* and *ABCG8* promotes biliary cholesterol secretion and reduces fractional absorption of dietary cholesterol. *J Clin Invest* 110, 671-680.

Yuan, Y.R., Blecker, S., Martsinkevich, O., Millen, L., Thomas, P.J., and Hunt, J.F. (2001). The crystal structure of the MJ0796 ATP-binding cassette. Implications for the structural consequences of ATP hydrolysis in the active site of an ABC transporter. *The Journal of biological chemistry* 276, 32313-32321.

Yvan-Charvet, L., Pagler, T., Gautier, E.L., Avagyan, S., Siry, R.L., Han, S., Welch, C.L., Wang, N., Randolph, G.J., Snoeck, H.W., and Tall, A.R. (2010a). ATP-binding cassette transporters and HDL suppress hematopoietic stem cell proliferation. *Science* 328, 1689-1693.

Yvan-Charvet, L., Ranalletta, M., Wang, N., Han, S., Terasaka, N., Li, R., Welch, C., and Tall, A.R. (2007). Combined deficiency of *ABCA1* and *ABCG1* promotes foam cell accumulation and accelerates atherosclerosis in mice. *J Clin Invest* 117, 3900-3908.

Yvan-Charvet, L., Wang, N., and Tall, A.R. (2010b). Role of HDL, ABCA1, and ABCG1 transporters in cholesterol efflux and immune responses. *Arteriosclerosis, thrombosis, and vascular biology* 30, 139-143.

Zhang, D.W., Cole, S.P., and Deeley, R.G. (2001a). Identification of a nonconserved amino acid residue in multidrug resistance protein 1 important for determining substrate specificity: evidence for functional interaction between transmembrane helices 14 and 17. *The Journal of biological chemistry* 276, 34966-34974.

Zhang, D.W., Cole, S.P., and Deeley, R.G. (2001b). Identification of an amino acid residue in multidrug resistance protein 1 critical for conferring resistance to anthracyclines. *The Journal of biological chemistry* 276, 13231-13239.

Zhang, D.W., Garuti, R., Tang, W.J., Cohen, J.C., and Hobbs, H.H. (2008). Structural requirements for PCSK9-mediated degradation of the low-density lipoprotein receptor. *Proceedings of the National Academy of Sciences of the United States of America* 105, 13045-13050.

Zhang, D.W., Graf, G.A., Gerard, R.D., Cohen, J.C., and Hobbs, H.H. (2006). Functional asymmetry of nucleotide-binding domains in ABCG5 and ABCG8. *The Journal of biological chemistry* 281, 4507-4516.

Zhang, D.W., Gu, H.M., Vasa, M., Muredda, M., Cole, S.P., and Deeley, R.G. (2003). Characterization of the role of polar amino acid residues within predicted transmembrane helix 17 in determining the substrate specificity of multidrug resistance protein 3. *Biochemistry* 42, 9989-10000.

Zhang, D.W., Lagace, T.A., Garuti, R., Zhao, Z., McDonald, M., Horton, J.D., Cohen, J.C., and Hobbs, H.H. (2007). Binding of proprotein convertase subtilisin/kexin type 9 to epidermal growth factor-like repeat A of low density lipoprotein receptor decreases receptor recycling and increases degradation. *The Journal of biological chemistry* 282, 18602-18612.

Appendices

Table 1 Primers for site mutagenesis

D319A	F: 5' - CAC AAC CCA GCA GCT TTT GTC ATG GAG - 3' R: 5' - CTC CAT GAC AAA AGC TGC TGG GTT GTG - 3'
F320A	F: 5' - CAC AAC CCA GCA GAT GCT GTC ATG GAG GTT - 3' R: 5' - AAC CTC CAT GAC AGC ATC TGC TGG GTT GTG - 3'
F320I	F: 5' - CCA GCA GAT ATT GTC ATG GAG GTT GCA TCC - 3' R: 5' - GGA TGC AAC CTC CAT GAC AAT ATC TGC TGG - 3'
F320Y	F: 5' - CCA GCA GAT TAT GTC ATG GAG GTT GCA TCC - 3' R: 5' - GGA TGC AAC CTC CAT GAC ATA ATC TGC TGG - 3'
N316A	F: 5' - CCA ACC TAC CAC GCC CCA GCA GAT TTT GTC - 3' R: 5' - GAC AAA ATC TGC TGG GGC GTG GTA GGT TGG - 3'
N316D	F: 5' - AAC TGC CCA ACC TAC CAC GAC CCA GCA GAT - 3' R: 5' - ATC TGC TGG GTC GTG GTA GGT TGG GCA GTT - 3'
N316Q	F: 5' - AAC TGC CCA ACC TAC CAC CAG CCA GCA GAT - 3' R: 5' - ATC TGC TGG CTG GTG GTA GGT TGG GCA GTT - 3'
P317A	F: 5' - ACC TAC CAC AAC GCA GCA GAT TTT GTC - 3' R: 5' - GAC AAA ATC TGC TGC GTT GTG GTA GGT - 3'
Y157A	F: 5' - CGG AAG GTG TCC TGC TTC ATC ATG CA - 3' R: 5' - ATC CTG CAT GAT GAA GCA GGA CAC CT - 3'
Q160A	F: 5' - TCC TGC TAC ATC ATG AAC GAT GAC AT - 3' R: 5' - CAG CAT GTC ATC GTT CAT GAT GTA GC - 3'

Table 2 QuikChange amplification reaction conditions

Steps	Cycles	Temperature	Time
1	1	95 °C	2 minutes
2	18	95 °C	30 seconds
		60 °C	10 seconds
		68 °C	2 minutes
3	1	68 °C	10 minutes